DISCRETE AND CONTINUOUS MODELS AND APPLIED COMPUTATIONAL SCIENCE

Volume 29 Number 2 (2021)

Founded in 1993
Founder: PEOPLES' FRIENDSHIP UNIVERSITY OF RUSSIA

DOI: 10.22363/2658-4670-2021-29-2

Edition registered by the Federal Service for Supervision of Communications, Information Technology and Mass Media
Registration Certificate: ПИ № ФС 77-76317, 19.07.2019

ISSN 2658-7149 (online); 2658-4670 (print)
4 issues per year.
Language: English.

Publisher: Peoples' Friendship University of Russia (RUDN University).
Indexed in Ulrich's Periodicals Directory (http://www.ulrichsweb.com), in https://elibrary.ru, EBSCOhost (https://www.ebsco.com), CyberLeninka (https://cyberleninka.ru).

Aim and Scope

Discrete and Continuous Models and Applied Computational Science arose in 2019 as a continuation of RUDN Journal of Mathematics, Information Sciences and Physics. RUDN Journal of Mathematics, Information Sciences and Physics arose in 2006 as a merger and continuation of the series "Physics", "Mathematics", "Applied Mathematics and Computer Science", "Applied Mathematics and Computer Mathematics".

Discussed issues affecting modern problems of physics, mathematics, queuing theory, the Teletraffic theory, computer science, software and databases development.

It's an international journal regarding both the editorial board and contributing authors as well as research and topics of publications. Its authors are leading researchers possessing PhD and PhDr degrees, and PhD and MA students from Russia and abroad. Articles are indexed in the Russian and foreign databases. Each paper is reviewed by at least two reviewers, the composition of which includes PhDs, are well known in their circles. Author's part of the magazine includes both young scientists, graduate students and talented students, who publish their works, and famous giants of world science.

The Journal is published in accordance with the policies of COPE (Committee on Publication Ethics). The editors are open to thematic issue initiatives with guest editors. Further information regarding notes for contributors, subscription, and back volumes is available at http://journals.rudn.ru/miph.

E-mail: miphj@rudn.ru, dcm@sci.pfu.edu.ru.

EDITORIAL BOARD

Computer Design: *A. V. Korolkova, D. S. Kulyabov*

Address of editorial board:
Ordzhonikidze St., 3, Moscow, Russia, 115419
Tel. +7 (495) 955-07-16, e-mail: publishing@rudn.ru
Editorial office:
Tel. +7 (495) 952-02-50, miphj@rudn.ru, dcm@sci.pfu.edu.ru
site: http://journals.rudn.ru/miph

Paper size 70×100/16. Offset paper. Offset printing. Typeface "Computer Modern".
Conventional printed sheet 5.80. Printing run 500 copies. Open price. The order 187.
PEOPLES' FRIENDSHIP UNIVERSITY OF RUSSIA
6 Miklukho-Maklaya St., 117198 Moscow, Russia
Printed at RUDN Publishing House:
3 Ordzhonikidze St., 115419 Moscow, Russia,
Ph. +7 (495) 952-04-41; e-mail: publishing@rudn.ru

Discrete & Continuous Models
& Applied Computational Science
2021, 29 (2) 104
http://journals.rudn.ru/miph

Contents

Discrete & Continuous Models & Applied Computational Science

2021, 29 (2) 105–113
http://journals.rudn.ru/miph

Research article

UDC 533.9
PACS 42.62.-b, 52.27.Ng, 52.35.Mw
DOI: 10.22363/2658-4670-2021-29-2-105-113

On the possibility of averaging the equations of an electron motion in the intense laser radiation

Vladimir P. Milant'ev

Peoples' Friendship University of Russia (RUDN University)
6, Miklukho-Maklaya St., Moscow 117198, Russian Federation

(received: March 12, 2021; accepted: May 25, 2021)

The problem of averaging of the relativistic motion equations of electron in the intense laser radiation, caused by the decreasing of the rate of wave phase change due to the Doppler's effect, is considered. As a result the phase can go from the "fast" to "slow" variables of the motion, so averaging over the phase becomes impossible. An analysis is presented of the conditions which are necessary for averaging of the relativistic equations of motion over the "fast" phase of the intense laser radiation on the base of the general principles of the averaging method. Laser radiation is considered in the paraxial approximation, where the ratio of the laser beam waist to the Rayleigh length is accepted as a small parameter. It is supposed that the laser pulse duration is of the order if the laser beam waist. In this case first-order corrections to the vectors of the laser pulse field should be taken into account. The general criterion for the possibility of the averaging of the relativistic motion equations of electron in the intense laser radiation is obtained. It is shown that an averaged description of the relativistic motion of an electron is possible in the case of a fairly moderate (relativistic) intensity and relatively wide laser beams. The known in the literature analogical criterion has been obtained earlier on the base of the numerical results.

Key words and phrases: intense laser pulse, relativistic electron, equations of motion, averaging of equations, criterion for averaged description of motion

1. Introduction

The nature of the motion of electrons in the field of electromagnetic waves substantially depends on the wave intensity, which is characterized by the dimensionless parameter $g = eE/\omega m_e c$. Here E is the electric field amplitude of the wave, ω is its angular frequency, e and m_e are the electron charge and mass, respectively, c is the velocity of light in vacuum. The first papers [1], [2] were devoted to the nonrelativistic motion of an electron in a high-frequency electromagnetic field of low intensity (parameter $g \ll 1$). It was shown by averaging over fast field oscillations, and expansions in terms of the parameter g, that the particle was subjected to the action of an averaged (ponderomotive) force. Later, the relativistic generalization of the ponderomotive force was considered under the condition that the parameter g was small [3], [4]. It was also noted that relativistic effects lead to various features of the averaged force [4]. In the field of high-power laser radiation, the parameter g is large ($g \geqslant 1$). So expansions in terms of the parameter g become impossible. In the case of electrons, the parameter $g = 1$, when the electric field strength E_r (V/cm) $= m_e c\omega/e = 3.21 \cdot 10^{10}/\lambda$ (μm), where λ (μm) is the wavelength. Radiation with electric field strength $E \geqslant E_r$ is called relativistically strong [5]. The parameter g is commonly represented in the form:

$$g = 0.855 \cdot 10^{-9} \lambda \sqrt{I}, \tag{1}$$

where $I = (cE^2/8\pi)$ [W/cm^2] is the intensity of the laser pulse. The parameter g is small in the case of a relatively weak field, when $I \ll I_r$. Here $I_r \equiv m_e^2 c^3 \omega^2 / 8\pi e^2$ is the relativistic intensity determined by the electric field strength E_r. Intensity of modern lasers can reach $I \geqslant 10^{18}$ W/cm^2 [6]–[8].

In the study of particle motion, an adequate description of the laser radiation field plays an important role. When describing laser radiation, the paraxial approximation and its modifications is often used [9]–[13] which are based on the expansion of field vectors in terms of a small parameter

$$\mu = a/Z_R \equiv 2/ka \ll 1. \tag{2}$$

Here a is the size of the laser beam in focus (beam waist), $Z_R = ka^2/2$ is the Rayleigh length, $k = 2\pi/\lambda = \omega/c$ is the wave number. We assume that the laser field propagates in the z-direction. From the Maxwell equations, one can find the expressions for the transverse components of the radiation field vectors $\mathbf{E}^0_{\perp m}$, $\mathbf{B}^0_{\perp m}$ of the zero approximation in the form of Gaussian beams of various modes m [9]–[13]. Longitudinal components E^1_{zm}, B^1_{zm} also arise, which are of the first-order quantities. The parameter (2) establishes the relation between the wavelength of radiation and the size of the focal spot. Powerful laser radiation also has a characteristic scale — the length (or duration Δt) of the pulse. In the case of extended pulses, the corrections to the transverse components of the radiation field are second-order quantities [9]. If the pulse length $c\Delta t$ and the size of the focal spot a are of the same order $c\Delta t \sim a$, then the first-order corrections to the transverse components of the field vectors $\mathbf{E}^1_{\perp m}$, $\mathbf{B}^1_{\perp m}$ appear [10]–[13]. In this case, the pulsed character of the radiation is specified by a fairly smooth pulse function $f(\sigma)$, where the parameter $\sigma = (t - z/c)/\Delta t$.

In the case of tightly focused laser radiation with the intensity $I \geqslant 10^{22}$ W/cm^2, the size of the focal spot can be equal to or smaller than the wavelength. In this case, the parameter (2) is not small, so that the paraxial approximation is not applicable and an exact solution of the Maxwell equations is necessary [14].

The presence of a small parameter (2) in the equations of the electron motion allows us to use the perturbation theory and perform averaging over fast oscillations of radiation. When they derive the ponderomotive force of a laser pulse, it is usually assumed that the wave amplitude varies slowly with respect to the wave phase (for example [15], [16]). However, the specific conditions for the relative change of these parameters are not considered. Meanwhile, the absence of such an analysis can lead to the misuse of averaging of the equations of motion. The fact is that during relativistic motion, the frequency of the radiation that the particle "sees" decreases due to the Doppler shift: $\omega' = \omega(1 - v_z/c)$. Here v_z is the component of the particle velocity in the direction of the laser pulse propagation. Doppler frequency shift slows down the rate of wave phase change. Therefore, at a sufficiently high longitudinal velocity of the particle, the rate of phase change may turn out to be comparable with the change in the wave amplitude. This problem was partially touched upon in the paper [4]. However, the conditions under which the averaging of the equations of motion is permissible were not discussed in detail. It was verified in the work [10] by numerical calculations that the domain of validity of the averaged description of the electron motion in the ultraintense laser pulse was given by the condition $1 - v_z/c \gg \varepsilon$, where $\varepsilon \equiv \mu/2$. However, the meaning of this condition and its validity was not discussed.

This paper is devoted to the detailed analysis of the conditions for averaging the relativistic equations of the electron motion in the field of high-power laser radiation with a sufficiently long pulse duration such that $\lambda \ll c\Delta t \sim a$. In this case, the existence of a small parameter (2) is assumed as in the work [10].

2. Basic relations

The motion of an electron is described by the following equations:

$$\begin{aligned}
\frac{dp_x}{dt} &= -(1 - v_z/c)eE_{xm} - eB^1_{zm}p_y/m_ec\gamma,\\
\frac{dp_y}{dt} &= -(1 - v_z/c)eE_{ym} + eB^1_{zm}p_x/m_ec\gamma,\\
\frac{dp_z}{dt} &= -eE^1_{zm} - e(p_xE_{xm} + p_yE_{ym})/m_ec\gamma,
\end{aligned} \tag{3}$$

$$\frac{d\mathbf{r}}{dt} = \frac{\mathbf{p}}{m_e\gamma}, \tag{4}$$

$$\frac{d\gamma}{dt} = -\frac{e}{(m_ec)^2\gamma}\mathbf{pE}. \tag{5}$$

Here $\mathbf{p} = (p_x, p_y, p_z)$ is the electron momentum vector, γ is the relativistic factor (dimensionless energy). The vectors of the laser field $\mathbf{E}_m$, $\mathbf{B}_m$ of an arbitrary mode m taking into account first-order terms are determined by the formulas [13] (or [10]). So $\mathbf{E}_m = \mathbf{E}^0_m + \mathbf{E}^1_m$ and $\mathbf{B}_m = \mathbf{B}^0_m + \mathbf{B}^1_m$. Along with the equations (3), it is necessary to use the equation for the wave phase θ:

$$\frac{d\theta}{dt} = -\omega(1 - v_z/c) \equiv -\omega G/\gamma. \tag{6}$$

Here

$$G \equiv \gamma - p_z/m_e c. \tag{7}$$

Let's note that the phase that the particle "senses" in the laser field differs from the phase θ by additional small terms [9]–[13]. However, in the case under consideration, these terms are not significant. The equations of motion (3) in the field of high-power laser radiation are very complicated for an analytical solution. Therefore, numerical methods of solution are often used that allow one to study some features of an electron motion in a laser field [10], [17]–[19]. In this case, most often, laser radiation is specified in the form of a Gaussian beam of the fundamental mode, even at $g \gg 1$, which, in general, is incorrect due to the following reasons: Solution of the Maxwell equations in the form of Gaussian (or Hermite–Gaussian) laser beams is the result of expansion of the field strength over the parameter (1). In the case of the ultra-intense and ultra-short laser pulses the size of the focal spot can be comparable with the wavelength [14]. So, the relation (1) is violated and description of the laser radiation in the form of the Gaussian beams becomes invalid. In this case exact solution of the Maxwell equations should be found [14].

3. Conditions for relativistic equations of motion averaging

A simplified description of electron interaction with a laser is achieved by averaging the equations of motion over the wave phase. Various versions of the averaged equations of motion have been considered in many works [20]–[24].

To average equations (3) over the phase θ, it must be a "rapidly" changing quantity [25]. It follows from the equation (6) that this depends on the difference $1 - v_z/c \equiv \Delta$, where $0 < \Delta \leqslant 1$ (if the particle moves in the direction of wave propagation). At $\Delta \sim 1$ the phase changes "quickly" and averaging over the phase is possible. The last is a general condition for averaging the equations of motion. In the ultrarelativistic limit ($\Delta \ll 1$) the phase θ becomes a "slow" (or "semi-fast") variable as well as the wave amplitude. In this case, the electron motion changes significantly and becomes more complicated [10]. In the presence of a unique small parameter (2), it is quite natural to present the above general averaging criterion in the modified form [10]:

$$\Delta \sim 1 \gg \mu. \tag{8}$$

It follows from (6), that the difference $\Delta = G/\gamma$, where the quantity G, according to equations (3), satisfies the equation:

$$\frac{dG}{dt} = e(1 - v_z/c)E^1_{xm}/m_e c + \dots . \tag{9}$$

One can see that the quantity G is an integral of motion only in the case of a plane electromagnetic wave in vacuum ($E^1_{zm} = 0$). In this case, the value G is determined by the initial conditions: $G = \gamma(0) - p_z(0)/m_e c$. If one considers the particles at rest at the initial instant of time, then $G = 1$. In the case of laser radiation, the longitudinal field E^1_{zm} always exists and plays an essential role in the motion of electrons. So, in general, the quantity G contains a slowly changing part as well as quickly oscillating corrections with small amplitudes. However, it is sometimes believed that $G = 1$ also in the case of laser radiation [11].

Let us further consider the averaging condition (8). In this case, the value G can be represented as the expansion in terms of the parameter μ:

$$G = G_0 + G_1 + \ldots, \tag{10}$$

where G_0 (the averaged value of the quantity G) does not depend on the wave phase θ, while G_i are periodic functions. According to equation (9), the quantity G_0 remains constant up to the first-order terms. It follows from the condition (8) that averaging of the equations of motion is possible if the following inequality is fulfilled:

$$\gamma\mu \ll G_0 \sim 1 \tag{11}$$

or

$$\gamma \ll 1/\mu = \pi a/\lambda. \tag{12}$$

This condition must be satisfied both during the injection of particles in the radiation field, and during their further movement. It follows from (11), (12) that an averaged description of motion is allowed when the energy of an accelerating particle is limited. Typically [10] the parameter $\mu < 6.4 \cdot 10^{-2}$. So the energy of the particle is restricted by the condition $\gamma \ll 17$.

Let us consider the relativistic factor $\gamma = \sqrt{1 + p^2/(mc)^2}$. With the definition (7), it is easy to obtain the following equation:

$$\gamma = [1 + G^2 + p_\perp^2/(m_e c)^2]/2G. \tag{13}$$

Here $p_\perp^2 = p_x^2 + p_y^2$. It follows from the system of equations (3) that $p_\perp \sim g m_e c$. Then from (13), we obtain the following estimate: $\gamma \sim 1 + g^2/2$. Given the inequality (12), we conclude that the averaging of electron motion equations in the field of relativistically intense laser radiation is possible if a rather stringent condition is satisfied:

$$1 + g^2/2 \ll \pi a/\lambda. \tag{14}$$

Thus, the averaging of the equations of motion is possible in the case of fairly moderate intensity of laser radiation and a relatively wide laser beam ($a/\lambda \gg 1$). In the case of ultra-intense radiation ($g \gg 1$), as it was already noted, the wavelength of the laser beam may be comparable with its size in the focus. Then the parameter in (2) turns out to be large, and expansion in the terms of this parameter becomes impossible. Moreover, at $g \gg 1$ the difference $1 - v_z/c \cong [1 + p_\perp^2/(m_e c)^2]/2\gamma^2 \sim g^{-2} \ll 1$, and motion of an electron becomes very complicated as it was noted in the paper [10]. That means that the concept of the relativistic ponderomotive force has rather restricted domain of validity.

4. Conclusion

It is shown that the condition $1 - v_z/c \gg \mu/2$, obtained by computer calculations in the paper [10], really corresponds to the general criterion (8) for averaging of the classical relativistic equations of electron motion in the intense laser beam. It leads to the conclusion that averaged description of the relativistic electron motion is possible at limited electron energy and limited intensity of the laser radiation, as it is established by the inequalities (12), (14). So averaging the equations of an electron motion over the wave phase seems to be possible in the case of a fairly moderate intensity and a relatively wide laser beam. Therefore, in general, it is impossible to consider the problem of the ponderomotive acceleration of electrons at very high intensity of the laser radiation. It should be particularly emphasized that for the averaging procedure it is necessary to take into account not only intensity but also other characteristics of the laser pulse.

Acknowledgement

The reported study was funded by RFBR, project No. 18-29-21041.

References

[1] H. Boot and R.-S. Harvie, "Charged particles in a non-uniform radiofrequency field," *Nature*, vol. 180, p. 1187, 1957. DOI: 10.1038/1801187a0.

[2] A. Gaponov and M. Miller, "Use of moving high-frequency potential wells for the acceleration of charged particles," *Soviet Physics JETP-USSR*, vol. 7, pp. 515–516, 1958.

[3] T. Kibble, "Mutual refraction of electrons and photons," *Physical Review*, vol. 150, p. 1060, 1966. DOI: 10.1103/PhysRev.150.1060.

[4] D. R. Bituk and M. V. Fedorov, "Relativistic ponderomotive forces," *JETP*, vol. 89, pp. 640–646, 4 1999. DOI: 10.1134/1.559024.

[5] G. A. Mourou, T. Tajima, and S. V. Bulanov, "Optics in the relativistic regime," *Reviews of Modern Physics*, vol. 78, p. 309, 2006. DOI: 10.1103/RevModPhys.78.309.

[6] N. M. Naumova, J. A. Nees, and G. A. Mourou, "Relativistic attosecond physics," *Physics of Plasmas*, vol. 12, p. 056 707, 2005. DOI: 10.1063/1.1880032.

[7] A. V. Korzhimanov *et al.*, "Horizons of petawatt laser technology," *Physics-Uspekhi*, vol. 54, p. 9, 2011. DOI: 10.3367/UFNe.0181.201101c.0009.

[8] C. Danson, D. Hillier, N. Hopps, and D. Neely, "Petawatt class lasers worldwide," *High Power Laser Science and Engineering*, vol. 3, 2015. DOI: 10.1017/hpl.2019.36.

[9] L. W. Davis, "Theory of electromagnetic beams," *Physical Review A*, vol. 19, pp. 1177–1179, 3 1979. DOI: 10.1103/PhysRevA.19.1177.

[10] B. Quesnel and P. Mora, "Theory and simulation of the interaction of ultraintense laser pulses with electrons in vacuum," *Physical Review E*, vol. 58, pp. 3719–3732, 3 1998. DOI: 10.1103/PhysRevE.58.3719.

[11] G. V. Stupakov and M. Zolotorev, "Ponderomotive laser acceleration and focusing in vacuum for generation of attosecond electron bunches," *Physical Review Letters*, vol. 86, p. 5274, 2001. DOI: 10.1103/PhysRevLett.86.5274.

[12] W. Wang, J. Xia L.and Xiong, H. Fang Z.and An, Z. Xie, W. Pei, and S. Fu, "Field shaping and electron acceleration by center-depressed laser beams," *Physics of Plasmas*, vol. 26, p. 093 109, 2019. DOI: 10.1063/1.5099508.

[13] V. P. Milant'ev, S. P. Karnilovich, and Y. N. Shaar, "Description of high-power laser radiation in the paraxial approximation," *Quantum Electronics*, vol. 45, pp. 1063–1068, 11 2015. DOI: 10.1070/QE2015V045N11ABEH015800.

[14] S. G. Bochkarev and V. Y. Bychenkov, "Acceleration of electrons by tightly focused femtosecond laser pulses," *Quantum Electronics*, vol. 37, pp. 273–284, 3 2007. DOI: 10.1070/QE2007v037n03ABEH013462.

[15] E. Startsev and C. McKinstrie, "Multiple scale derivation of the relativistic ponderomotive force," *Physical Review E*, vol. 55, p. 7527, 1997. DOI: 10.1103/PhysRevE.55.7527.

[16] P. Mora and J. T. M. Antonsen, "Kinetic modeling of intense, short laser pulses propagating in tenuous plasmas," *Physics of Plasmas*, vol. 4, pp. 217–229, 1997. DOI: 10.1063/1.872134.

[17] Y. I. Salamin, G. R. Mocken, and C. H. Keitel, "Electron scattering and acceleration by a tightly focused laser beam," *Physical Review Special Topics-Accelerators and Beams*, vol. 5, p. 101 301, 2002. DOI: 10.1103/PhysRevSTAB.5.101301.

[18] P. Wang *et al.*, "Characteristics of laser-driven electron acceleration in vacuum," *Journal of Applied Physics*, vol. 91, pp. 856–866, 2002. DOI: 10.1063/1.1423394.

[19] A. Galkin, V. Korobkin, M. Y. Romanovsky, and O. Shiryaev, "Dynamics of an electron driven by relativistically intense laser radiation," *Physics of Plasmas*, vol. 15, p. 023 104, 2008. DOI: 10.1063/1.2839349.

[20] D. Bauer, P. Mulser, and W. H. Steeb, "Relativistic ponderomotive force, uphill acceleration and transition to chaos," *Physical Review Letters*, vol. 75, pp. 4622–4625, 25 1995. DOI: 10.1103/PhysRevLett.75.4622.

[21] I. Y. Dodin, N. J. Fisch, and G. M. Fraiman, "Drift lagrangian for a relativistic particle in an intense laser field," *Journal of Experimental and Theoretical Physics Letters*, vol. 78, pp. 202–206, 2003. DOI: 10.1134/1.1622032.

[22] N. B. Narozhny and M. S. Fofanov, "Scattering of relativistic electrons by a focused laser pulse," *JETP*, vol. 90, pp. 753–768, 5 2000. DOI: 10.1134/1.559160.

[23] A. J. Castillo and V. P. Milant'ev, "Relativistic ponderomotive forces in the field of intense laser radiation," *Technical Physics*, vol. 59, pp. 1261–1266, 9 2014. DOI: 10.1134/S1063784214090138.

[24] V. P. Milant'ev and A. J. Castillo, "On the theory of the relativistic motion of a charged particle in the field of intense electromagnetic radiation," *JETP*, vol. 116, pp. 558–566, 4 2013. DOI: 10.1134/S1063776113040067.

[25] N. N. Bogoljubov and Y. A. Mitropolskij, *Asymptotic methods in the theory of nonlinear oscillations.* New York: CRC Press, 1961, vol. 10, p. 537. DOI: 10.1007/BF01056172.

For citation:
V. P. Milant'ev, On the possibility of averaging the equations of an electron motion in the intense laser radiation, Discrete and Continuous Models and Applied Computational Science 29 (2) (2021) 105–113. DOI: 10.22363/2658-4670-2021-29-2-105-113.

Information about the authors:
Vladimir P. Milant'ev — Doctor of Physical and Mathematical Sciences, Professor of Institute of Physical Research and Technology of Peoples' Friendship University of Russia (RUDN University) (e-mail: milantiev-vp@rudn.ru, phone: +7(499) 2483057, ORCID: https://orcid.org/0000-0003-4686-4229, ResearcherID: B-9335-2016, Scopus Author ID: 6602468700)

УДК 533.9
PACS 42.62.-b, 52.27.Ng, 52.35.Mw
DOI: 10.22363/2658-4670-2021-29-2-105-113

О возможности усреднения релятивистских уравнений движения электрона в поле мощного лазерного излучения

В. П. Милантьев

Российский университет дружбы народов
ул. Миклухо-Маклая, д. 6, Москва, 117198, Россия

Рассмотрена проблема усреднения релятивистских уравнений движения электрона в поле мощного лазерного излучения, вызванная уменьшением скорости изменения фазы волны из-за эффекта Доплера. Вследствие этого фаза может перейти из числа «быстрых» в число «медленных» переменных движения, так что усреднение по фазе становится невозможным. На основе общих принципов метода усреднения проведён анализ условий, при которых допустимо усреднение уравнений движения по «быстрой» фазе излучения. Лазерное излучение рассматривается в параксиальном приближении, в котором малым параметром является отношение сужения лазерного пучка к рэлеевской длине. Предполагается, что протяжённость импульса сопоставима с порядком сужения лазерного пучка. В этом случае необходимо учитывать поправки первого порядка к векторам поля лазерного импульса. Получен общий критерий, определяющий возможность усреднения релятивистских уравнений движения частицы в поле мощного лазерного излучения. Показано, что усреднённое описание релятивистского движения электрона возможно в случае достаточно умеренной (релятивистской) интенсивности и относительно широких лазерных пучков. Известный в литературе аналогичный критерий был получен ранее на основе численных расчётов.

Ключевые слова: мощный лазерный импульс, релятивистский электрон, уравнения движения, усреднение уравнений, критерий для усреднённого описания движения

Research article

UDC 519.872:519.217
PACS 07.05.Tp, 02.60.Pn, 02.70.Bf
DOI: 10.22363/2658-4670-2021-29-2-114-125

Investigation of the existence domain for Dyakonov surface waves in the Sage computer algebra system

Oleg K. Kroytor

Peoples' Friendship University of Russia (RUDN University)
6, Miklukho-Maklaya St., Moscow, 117198, Russian Federation

(received: March 25, 2021; accepted: May 25, 2021)

Surface electromagnetic waves (Dyakonov waves) propagating along a plane interface between an isotropic substance with a constant dielectric constant and an anisotropic crystal, whose dielectric tensor has a symmetry axis directed along the interface, are considered. It is well known that the question of the existence of such surface waves is reduced to the question of the existence of a solution to a certain system of algebraic equations and inequalities. In the present work, this system is investigated in the Sage computer algebra system.

The built-in technique of exceptional ideals in Sage made it possible to describe the solution of a system of algebraic equations parametrically using a single parameter, with all the original quantities expressed in terms of this parameter using radicals. The remaining inequalities were only partially investigated analytically. For a complete study of the solvability of the system of equations and inequalities, a symbolic-numerical algorithm is proposed and implemented in Sage, and the results of computer experiments are presented. Based on these results, conclusions were drawn that require further theoretical substantiation.

Key words and phrases: surface waves, Dyakonov waves, electromagnetic waves, computer algebra, Sage

1. Introduction

In the 1980s, a special class of solutions to Maxwell's equations was theoretically discovered, namely, electromagnetic waves traveling along the interface between two dielectrics, the intensity of which rapidly decreases with distance from the interface [1]–[6]. These waves are called Dyakonov surface waves. Experimental observation of surface waves was carried out quite recently [7], [8]. In theoretical works, as in the work of Dyakonov itself [2], the question of the existence of surface waves was reduced to the question of the existence of a solution to a certain system of algebraic equations and inequalities that cannot be solved analytically, which hinders further research. In this paper, it will be shown what computer algebra systems can give for these systems.

2. Surface waves

We investigate the classical problem of waves propagating along the interface of an anisotropic medium with permittivity

$$\epsilon = \mathrm{diag}(\epsilon_o, \epsilon_o, \epsilon_e)$$

and isotropic medium with constant permittivity ϵ. For definiteness, let the plane $x = 0$ serve as an interface. The field in the anisotropic medium ($x < 0$) is sought in the form

$$\vec{E} = \left(a_o\vec{E}_o e^{p_o x} + a_e\vec{E}_e e^{p_e x}\right) e^{ik_y y + ik_z z - i\omega t},$$
$$\vec{H} = \left(a_o\vec{H}_o e^{p_o x} + a_e\vec{H}_e e^{p_e x}\right) e^{ik_y y + ik_z z - i\omega t}.$$

Here ω is the circular frequency of the wave, $k_0 = \omega/c$ is the wave number, $\vec{k}_\perp = (0, k_y, k_z)$ is its wave vector, a_o, a_e are the amplitudes of two partial waves, and positive numbers p_o, p_e characterize the rate of wave decay in the anisotropic medium. Maxwell's equations give

$$\begin{aligned} p_o^2 &= k_y^2 + k_z^2 - \epsilon_o k_0^2, \\ p_e^2 &= k_y^2 + \frac{\epsilon_e}{\epsilon_o} k_z^2 - \epsilon_e k_0^2 \end{aligned} \tag{1}$$

and for the vectors $\vec{E}_o, \dots, \vec{H}_e$, explicit expressions are obtained, which we will not present here.

For the isotropic medium ($x > 0$) the field is described by similar formulas

$$\vec{E} = \left(b_o\vec{E}'_o + b_e\vec{E}'_e\right) e^{-px} e^{ik_y y + ik_z z - i\omega t},$$
$$\vec{H} = \left(b_o\vec{H}'_o + b_e\vec{H}'_e\right) e^{-px} e^{ik_y y + ik_z z - i\omega t},$$

but now the constant p, which characterizes the field decrease in the isotropic medium, turns out to be the same:

$$p^2 = k_y^2 + k_z^2 - \epsilon k_0^2. \tag{2}$$

The conditions for matching electromagnetic fields at the interface lead to a system of homogeneous linear equations for the amplitudes a_o, a_e, b_o, b_e. The condition of zero determinant of this system gives the equation

$$\begin{aligned} \big((k_z^2 - \epsilon k_0^2)p_o + (k_z^2 - \epsilon_o k_0^2)p\big)\big((k_z^2 - \epsilon k_0^2)\epsilon_o p_e + (k_z^2 - \epsilon_o k_0^2)\epsilon p\big) = \\ = (\epsilon_o - \epsilon)^2 k_y^2 k_z^2 k_0^2. \end{aligned} \tag{3}$$

If real parameters k_y, k_z, p_o, p_e and p satisfy four algebraic equations (1), (2) and (3), then we get a solution to Maxwell's equations in the integral form defined in the entire space. These solutions exponentially decrease at $|x| \to \infty$, if the solution is in the domain

$$p_o > 0, \quad p_e > 0, \quad p > 0 \tag{4}$$

of five-dimensional space $k_y k_z p_o p_e p$.

The existence of solution to this system does not ensure that the resulting field is not identically zero, an example will be given below. This issue requires additional check.

3. Investigation of the system of algebraic equations

Consider in more detail the above system of four algebraic equations (1), (2), and (3).

It is possible to eliminate k_0 from this system by assuming

$$p = k_0 q, \quad p_o = k_0 q_o, \quad p_e = k_0 q_e$$

and $k_y = k_0 \beta$, $k_z = k_0 \gamma$.

Then the system of equations is written in the form

$$\begin{cases} q_o^2 = \beta^2 + \gamma^2 - \epsilon_o, \\ q_e^2 = \beta^2 + \dfrac{\epsilon_e}{\epsilon_o}\gamma^2 - \epsilon_e, \\ q^2 = \beta^2 + \gamma^2 - \epsilon, \\ \big((\gamma^2 - \epsilon)q_o + (\gamma^2 - \epsilon_o)q\big)\big((\gamma^2 - \epsilon)\epsilon_o q_e + (\gamma^2 - \epsilon_o)\epsilon q\big) = \\ = (\epsilon_o - \epsilon)^2 \beta^2 \gamma^2. \end{cases} \tag{5}$$

This is a system of 4 equations for 5 unknowns, so you can exclude 3 unknowns from it and find a connection between the remaining two. Since for applications the direction of the vector $\vec{k}_\perp$, that is, the ratio of β and γ, is most interesting, it is quite natural to try to exclude the quantities q, q_o, q_e, which characterize the rate of decay of the solution with distance from surface $x = 0$. However, in this way, a very complex equation is obtained, which then has to be investigated numerically.

However, it is easy to see that the unknowns β and γ enter the system only as squares, so it is convenient to exclude them. We did not do it by hand, but used the technique of exceptional ideals [9], implemented in the Sage computer algebra system **Sage**. We have eliminated the unknowns β, γ, q, and obtained an equation of the form $F(q_o, q_e) = 0$, whose coefficients depend only on permittivities. The right-hand side of this equation can be represented as a product of three factors. Consider each of them separately.

First, system (5) has a solution with $q_e = q_o$. Then the difference of the first two equations of system (5) yields

$$\frac{\epsilon_e - \epsilon_o}{\epsilon_o}\gamma^2 - (\epsilon_e - \epsilon_o) = 0$$

or $\gamma^2 = \epsilon_o$.

Such a solution really exists, but on it $k_z^2 - \epsilon_o k_0^2 = 0$, so that $b_o = b_e = 0$ (the field in the isotropic medium is zero) and $\vec{E}_o$ and $\vec{E}_e$ become linearly dependent. Therefore, even at nonzero a_o, a_e the field in the anisotropic medium can be zero. From general considerations it is obvious that it is just so in the case considered: the field cannot flow from the anisotropic medium.

The second factor yields

$$(q_e^2 - q_o^2)\epsilon_o = (\epsilon - \epsilon_o)(\epsilon_e - \epsilon_o).$$

The difference of first two equations of system (5) yields

$$(q_e^2 - q_o^2)\epsilon_o = (\epsilon_e - \epsilon_o)(\gamma^2 - \epsilon_o).$$

Therefore, $\gamma^2 = \epsilon$. This is the second trivial case: now $a_o = a_e = 0$ and the field is absent in the anisotropic medium.

Ignoring trivial fields, we see that system (5) has a solution if and only if the third factor turns into zero:

$$\begin{aligned} - q_o^4\epsilon^2 - 2q_o^3 q_e\epsilon^2 - q_o^2q_e^2\epsilon^2 - 2q_o^2q_e^2\epsilon\epsilon_o - 2q_oq_e^3\epsilon\epsilon_o + q_o^2q_e^2\epsilon_o^2 - q_e^4\epsilon_o^2 + \\ + 2q_o^4\epsilon\epsilon_e + 2q_o^3q_e\epsilon\epsilon_e + 2q_o^3q_e\epsilon_o\epsilon_e + 2q_o^2q_e^2\epsilon_o\epsilon_e - \\ - q_e^2\epsilon\epsilon_o^2 + q_e^2\epsilon_o^3 - 2q_oq_e\epsilon\epsilon_o\epsilon_e + 2q_oq_e\epsilon_o^2\epsilon_e - q_o^2\epsilon\epsilon_e^2 + q_o^2\epsilon_o\epsilon_e^2 = 0. \end{aligned} \quad (6)$$

This expression is somewhat cumbersome, however, its structure is easily seen

$$F_4(q_o, q_e) + F_2(q_o, q_e) = 0,$$

where F_4, F_2 are homogeneous functions of the 4-th and 2-nd order $q_e = tq_o$, so that we rewrite this equation as

$$q_o^2 F_4(1,t) + F_2(1,t) = 0.$$

Hence

$$q_o = \sqrt{\frac{-F_2(1,t)}{F_4(1,t)}},$$

where t can take any values.

The theory of exclusive ideals applied above yields an equation

$$F(q_o, q_e) = 0$$

as a necessary and sufficient condition for the existence of a solution to system (5), but this solution can be complex and infinitely large [9]. In this case one can express the solution in terms of parameter t in radicals. Thus, the investigation of solvability of the system of algebraic equations reduced to an investigation of one equation solved in radicals.

Quantities q_e and q are rather simply expressed via t and q_o: by definition

$$q_e = tq_o,$$

and due to the first and the third equation of system (5)

$$q^2 = q_o^2 + \epsilon_o - \epsilon. \tag{7}$$

The quantities β^2, γ^2 can be reconstructed by solving the system of equations linear with respect to β^2, γ^2

$$\begin{cases} \beta^2 + \gamma^2 = q_o^2 + \epsilon_o, \\ \epsilon_o \beta^2 + \epsilon_e \gamma^2 = \epsilon_o q_e^2 + \epsilon_o \epsilon_e \end{cases}$$

formed by the first and the second equation of system (5). Solving it we get

$$\beta^2 = \frac{(\epsilon_e - \epsilon_o t^2) q_o^2}{\epsilon_e - \epsilon_o} \tag{8}$$

and

$$\gamma^2 = \frac{\epsilon_o \big(\epsilon_e - \epsilon_o + (t^2 - 1) q_o^2\big)}{\epsilon_e - \epsilon_o}. \tag{9}$$

The issue of extracting radicals is not trivial here. From the general theory, we know that at least one choice of the root branch should result in a solution. Since only squares of β, γ enter system (5), the solution will be obtained for any choice of signs before the radicals. However, q enters the system in the first power, so that the solution of system (5) can and as we will see below will be obtained for the only choice of the branch choice for the root when calculating the value of q from (7).

4. Investigation of the system of algebraic equations and inequalities

As was noted in [2], for the existence of surface waves the fulfillment of condition

$$0 < \epsilon_o < \epsilon < \epsilon_e \tag{10}$$

is necessary. To avoid special consideration of the cases when there are deliberately no surface waves, we present here an analysis of the issue of fulfilment of inequalities

$$q_o > 0, \quad q_e > 0, \quad q > 0 \tag{11}$$

only for the Dyakonov case (10). If the first two inequalities are satisfied, then $t = q_e/q_o$ is positive. Therefore, below we restrict ourselves by considering only positive values of parameter t.

So, let t have a positive value, and a solution of system (5) has been constructed using the formulas of the previous section. In order q_o be positive, the fulfillment of the following inequality is necessary and sufficient:

$$\frac{-F_2(1,t)}{F_4(1,t)} > 0. \tag{12}$$

This value itself can be found from

$$q_o = \sqrt{\frac{-F_2(1,t)}{F_4(1,t)}}.$$

In this case, $q_e = tq_o$ also has a positive value.

Since $F_2(q_o, q_e)$ and $F_4(q_o, q_e)$ are terms of the second and fourth order in expression (6), we can write the radicand explicitly:

$$F_2(1,t) = -(\epsilon_o t + \epsilon_e)^2(\epsilon - \epsilon_o),$$

and

$$F_4(1,t) = -(\epsilon_o t^2 + (\epsilon - \epsilon_o)t + \epsilon - 2\epsilon_e)(\epsilon_o t + \epsilon)(t+1).$$

This means that in the Dyakonov case $-F_2 > 0$ and the sign of ratio F_2/F_4 is determined by the sign of factor

$$\epsilon_o t^2 + (\epsilon - \epsilon_o)t + \epsilon - 2\epsilon_e.$$

The discriminant of this quadratic trinomial equals

$$D = \epsilon^2 + \epsilon_o^2 + 2\epsilon_o(4\epsilon_e - 3\epsilon) > 0,$$

therefore, its roots are real. Since $\epsilon - 2\epsilon_e < 0$, these roots have different signs. Let us denote the positive root as

$$t_1 = \frac{\epsilon_o - \epsilon + \sqrt{D}}{2\epsilon_o}.$$

The expression $-F_2/F_4$ will be positive if and only if

$$0 < t < t_1. \tag{13}$$

For the square of quantity β, calculated from (8) to be positive, it is necessary and sufficient that

$$t < \sqrt{\frac{\epsilon_e}{\epsilon_o}}$$

was valid. For the square of quantity q, calculated from (7) to be positive, it is necessary and sufficient that the condition

$$q_o^2 > \epsilon - \epsilon_o$$

or

$$\frac{-F_2(1,t)}{F_4(1,t)} > \epsilon - \epsilon_o \tag{14}$$

was satisfied.

In the Dyakonov case $-F_2 > 0$ and provided that the inequality (13) is fulfilled, the expression $F_4 > 0$, therefore inequality (14) can be rewritten as

$$-F_2(1,t) > (\epsilon - \epsilon_o)F_4(1,t)$$

or

$$(\epsilon_o t + \epsilon_e)^2 > -(\epsilon_o t^2 + (\epsilon - \epsilon_o)t + \epsilon - 2\epsilon_e)(\epsilon_o t + \epsilon)(t+1). \tag{15}$$

For the square of the value γ calculated by the formulas (9) to be positive, it is necessary and sufficient that

$$(1-t^2)q_o^2 > \epsilon_e - \epsilon_o$$

or

$$(1-t^2)(\epsilon_o t + \epsilon_e)^2 > -(\epsilon_o t^2 + (\epsilon - \epsilon_o)t + \epsilon - 2\epsilon_e)(\epsilon_o t + \epsilon)(t+1). \tag{16}$$

To summarize what has been said: the solution of system (5) obtained by the parametric formulas written out falls into the region (11) if and only if

1) the parameter t belongs to the interval

$$0 < t < \min\left(t_1, \sqrt{\frac{\epsilon_e}{\epsilon_o}}\right); \tag{17}$$

2) two inequalities (15) and (16) are satisfied, and

3) the last equation of system (5) is valid for the choice of the radical principal value.

The fulfillment of these conditions can be checked in the Sage system.

Example. Let $\epsilon_o = 2$, $\epsilon = 3$, $\epsilon_e = 5$. Figure 1 presents a plot of q_o (black line) at the values of parameter t, taken from the interval (17), dash lines indicate the boundaries of the domain of t, q_o variation, determined by inequalities (15) and (16). The restrictions of t are seen to automatically provide the fulfillment of conditions for q_o. There is the only point $t = 1/2$, where the plot touches the lower boundary. Just at this point the expression for q changes its sign. Figure 2 presents the plot of the right-hand side of the last equation for the chosen sign '+': up to the point $t = 1/2$ we get a solution, and after this point not. Therefore, the solution satisfies the condition $q > 0$ only at $0 < t < 1/2$.

For these values β and γ were calculated which appeared to be real-valued. For clarity, figure 3 presents a plot of dependence of t on the angle u, expressed as

$$\frac{\gamma}{\beta} = \frac{k_z}{k_y} = \tan u.$$

It turns out that the surface wave arises only in the directions

$$\vec{k}_\perp = (0, k_y, k_z)^T,$$

within a narrow range of angles 38–45°.

This example shows that 1) inequalities (15) and (16) are fulfilled in the entire considered interval of parameter t variation, and 2) upon the choice of principal value for the radical our explicit formulae yield a solution to system (5) only up to the point where the plot of q_o touches the lower boundary of its corridor. We believe that these assertions can be proved in a purely algebraic way.

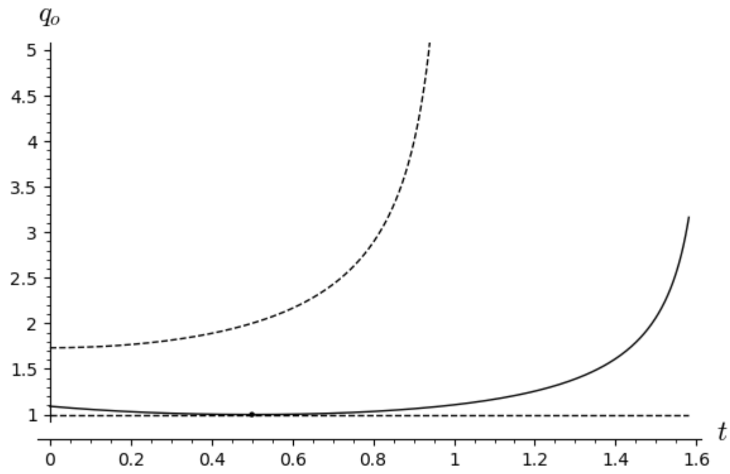

Figure 1. Plot of q_o (black line), dash lines indicate the boundaries of the domain of t, q_o variation

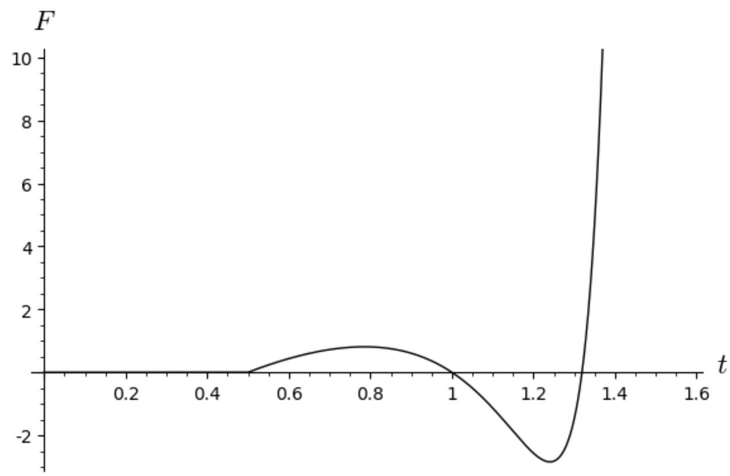

Figure 2. Plot of the left-hand side of the last of equations (5)

5. Results of computer experiments

We conducted a series of computer experiments, the results of which are given in the table 1. Based on them, we can draw the following conclusions:

1) the greater the difference between ϵ and ϵ_e, and the smaller it is between the values ϵ_o and ϵ, the greater the half-width of the interval for changing the angle u (see the table 1 cases numbered 12 and 13);
2) the smaller the difference between ϵ and ϵ_e, and the larger it is between the values ϵ_o and ϵ_e, the smaller the half-interval of the angle u (see the table 1 cases numbered 14 and 15);

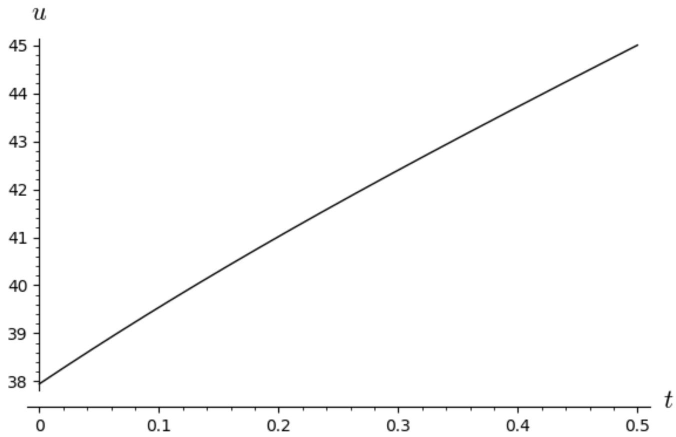

Figure 3. Plot of u, the angle is in degrees

3) if the difference between the values ϵ_o, ϵ, ϵ_e remains constant, and the values themselves increase, then the half-interval of the angle u variation, in which surface waves exist, decreases (see the table 1, cases numbered 4, 16, 17, 18);
4) if the difference between the values of ϵ_o, ϵ, ϵ_e is increased by the same amount, the half-interval of u variation is practically unchanged (see the table 1, cases 19–21).

These conclusions are awaiting theoretical substantiation.

We failed to find a simple relationship between the position of the mean angle u and the values of ϵ_o, ϵ, ϵ_e, while the position of the mean angle u itself changes quite noticeably.

To test our approach, we looked at several non-Dyakonov cases where one of the (10) inequalities is violated. As expected, no solutions were found in these cases.

6. Conclusion

Investigation of the region of existence of the Dyakonov surface wave at the isotropic-anisotropic interface is reduced to a system of algebraic equations and inequalities. We managed to solve this system of equations in radicals in the Sage computer algebra system. At the same time, the inequalities were only partially investigated analytically. On this basis, it was possible to carry out a series of computer experiments clarifying further directions of research.

Acknowledgments

The author thanks Prof. L. A. Sevastyanov and M. D. Malykh (RUDN University) for setting an interesting problem and permanent attention to his work. All calculations presented in the article were performed in the Sage system **Sage**. The publication was supported by the RUDN University Strategic Academic Leadership Program.

Table 1

Results of computer experiments

No.	ϵ_o	ϵ	ϵ_e	Mean angle u, deg.	Half-interval of angle u variation, deg.
1	1	2	3	27 – 34	3.5
2	2	3	5	38 – 45	3.5
3	2.5	3.5	5.5	40.5 – 47	3.25
4	3	4	6	42.4 – 48.5	3.05
5	3	4	10	45.6 – 53.8	4.1
6	3.0001	3.001	3.01	72.426 – 72.455	0.0145
7	3	3.01	3.02	44.911 – 45	0.0445
8	3	4	4.001	1.57 – 1.76	0.095
9	3.9	4	4.1	44.299 – 44.96	0.3305
10	3.9	4	4.001	5.649 – 5.71	0.0305
11	3.99	4	4.001	17.522 – 17.548	0.013
12	2	7	55	13.2 – 19.2	3
13	2	2.1	80	45.47 – 56	5.265
14	2	54	55	1.5 – 2.22	0.36
15	2	79.9	80	0.3275 – 0.4825	0.155
16	13	14	16	51.5 – 53.58	1.04
17	33	34	36	53.59 – 54.46	0.435
18	133	134	136	54.446 – 54.78	0.167
19	20	40	60	27 – 34	3.5
20	20	50	80	23 – 30	3.5
21	20	60	100	20.2 – 27.2	3.5

References

[1] F. N. Marchevskii, V. L. Strizhevskii, and S. V. Strizhevskii, "Singular electromagnetic waves in bounded anisotropic media," *Sov. Phys. Solid State*, vol. 26, p. 857, 1984.

[2] M. I. Dyakonov, "New type of electromagnetic wave propagating at an interface," *Sov. Phys. JETP*, vol. 67, p. 714, 1988.

[3] O. Takayama, L.-C. Crasovan, S. Johansen, D. Mihalache, D. Artigas, and L. Torner, "Dyakonov surface waves: a review," *Electromagnetics*, vol. 28, pp. 126–145, 2008. DOI: 10.1080/02726340801921403.

[4] J. A. Polo Jr. and A. Lakhtakia, "A Surface Electromagnetic Waves: a Review," *Laser & Photonics Reviews*, vol. 5, pp. 234–246, 2011. DOI: 10.1002/lpor.200900050.

[5] O. N. Bikeev and L. A. Sevastianov, "Surface electromagnetic waves at the interface of two anisotropic media," *RUDN Journal of Mathematics, Information Sciences and Physics*, vol. 25, no. 2, pp. 141–148, 2017, in Russian. DOI: 10.22363/2312-9735-2017-25-2-141-148.

[6] O. N. Bikeev, K. P. Lovetskiy, N. E. Nikolaev, L. A. Sevastianov, and A. A. Tiutiunnik, "Electromagnetic surface waves guided by a twist discontinuity in a uniaxial dielectric with optic axis lying in the discontinuity plane," *Journal of Electromagnetic Waves and Applications*, vol. 33, no. 15, pp. 2009–2021, 2017. DOI: 10.1080/09205071.2019.1655486.

[7] O. Takayama, L.-C. Crasovan, D. Artigas, and L. Torner, "Observation of Dyakonov surface waves," *Physical Review Letters*, vol. 102, p. 043 903, 2009. DOI: 10.1103/PhysRevLett.102.043903.

[8] O. Takayama, D. Artigas, and L. Torner, "Lossless directional guiding of light in dielectric nanosheets using Dyakonov surface waves," *Nature Nanotech*, vol. 9, pp. 419–424, 2014. DOI: 10.1038/nnano.2014.90.

[9] D. Cox, J. Little, and D. O'Shea, *Ideals, varieties, and algorithms*, 2nd ed. Springer, 1997.

For citation:

O. K. Kroytor, Investigation of the existence domain for Dyakonov surface waves in the Sage computer algebra system, Discrete and Continuous Models and Applied Computational Science 29 (2) (2021) 114–125. DOI: 10.22363/2658-4670-2021-29-2-114-125.

Information about the authors:

Kroytor, Oleg K. — Postgraduate of Department of Applied Probability and Informatics of Peoples' Friendship University of Russia (RUDN University); (e-mail: kroytor_ok@pfur.ru, phone: +7(495)9550927, ORCID: https://orcid.org/0000-0002-5691-7331)

УДК 519.872:519.217
PACS 07.05.Tp, 02.60.Pn, 02.70.Bf
DOI: 10.22363/2658-4670-2021-29-2-114-125

Исследование области существования поверхностных волн Дьяконова в системе компьютерной алгебры Sage

О. К. Кройтор

Российский университет дружбы народов
ул. Миклухо-Маклая, д. 6, Москва, 117198, Россия

Рассмотрены поверхностные электромагнитные волны (волны Дьяконова), распространяющиеся вдоль плоской границы раздела изотропного вещества с постоянной диэлектрической проницаемостью, и анизотропного кристалла, тензор диэлектрической проницаемости которого имеет ось симметрии, направленную вдоль границы раздела. Хорошо известно, что вопрос о существовании таких поверхностных волн сводится к вопросу о существовании решения некоторой системы алгебраических уравнений и неравенств. В настоящей работе эта система исследована в системе компьютерной алгебры Sage.

Техника исключительных идеалов, встроенная в Sage, позволила описать решение системы алгебраических уравнений параметрически при помощи одного параметра, причём все исходные величины выражаются через этот параметр при помощи радикалов. Оставшиеся неравенства удалось исследовать аналитически лишь частично. Для полного исследования разрешимости системы уравнений и неравенств предложен и реализован в Sage символьно-численный алгоритм, представлены результаты компьютерных экспериментов. На основе результатов экспериментов были сделаны выводы, которые требуют дальнейшего теоретического обоснования.

Ключевые слова: поверхностные волны, волны Дьяконова, электромагнитные волны, компьютерная алгебра, Sage

Research article

UDC 517.928.1:517.958:519.633
PACS 02.30.Jr, 02.30.Mv, 11.10.Jj, 05.20.Dd, 05.40.Jc,
DOI: 10.22363/2658-4670-2021-29-2-126-145

The asymptotic solution of a singularly perturbed Cauchy problem for Fokker–Planck equation

Mohamed A. Bouatta[1], **Sergey A. Vasilyev**[1], **Sergey I. Vinitsky**[1,2]

[1] *Peoples' Friendship University of Russia (RUDN University)*
6, Miklukho-Maklaya St., Moscow, 117198, Russian Federation
[2] *Joint Institute for Nuclear Research*
6, Joliot-Curie St., Dubna, Moscow Region, 141980, Russian Federation

(received: March 31, 2021; accepted: May 25, 2021)

The asymptotic method is a very attractive area of applied mathematics. There are many modern research directions which use a small parameter such as statistical mechanics, chemical reaction theory and so on. The application of the Fokker–Planck equation (FPE) with a small parameter is the most popular because this equation is the parabolic partial differential equations and the solutions of FPE give the probability density function.

In this paper we investigate the singularly perturbed Cauchy problem for symmetric linear system of parabolic partial differential equations with a small parameter. We assume that this system is the Tikhonov non-homogeneous system with constant coefficients. The paper aims to consider this Cauchy problem, apply the asymptotic method and construct expansions of the solutions in the form of two-type decomposition. This decomposition has regular and border-layer parts. The main result of this paper is a justification of an asymptotic expansion for the solutions of this Cauchy problem. Our method can be applied in a wide variety of cases for singularly perturbed Cauchy problems of Fokker–Planck equations.

Key words and phrases: asymptotic analysis, singularly perturbed differential equation, Cauchy problem, Fokker–Planck equation

1. Introduction

It is well known that the differential operator, which is applied in the theory of measure, has such form:

$$L = a^{ij}\partial_{x_i}\partial_{x_j} + b^i\partial_{x_i}, \quad 1 \leqslant i, j \leqslant d, \quad d \in N.$$

The solution of the equation $L^*\mu = 0$ is Borel measures on an open set $\Omega \in \mathbf{R}^d$ and there is the relation

$$\int_\Omega Lf d\mu = 0, \quad \forall f \in C_0^\infty(\Omega).$$

If the measure μ has a density ρ, then ρ is conjugate solution of the equation

$$\partial_{x_i}\partial_{x_j}a^{ij}\rho(x) - \partial_{x_i}b^i\rho(x) = 0, \quad x \in \Omega.$$

Similarly, we can consider parabolic operators in the form

$$P = \partial_t - \partial_{x_i}\partial_{x_j}a^{ij} + \partial_{x_i}b^i,$$

and there are appropriate parabolic equations $P^*\mu = 0$ for finding measures μ on $\mathbf{R}^n \times [0,T]$. The equations for the study of density have the form of Fokker–Planck equation (FPE)

$$\partial_t\rho(x,t) - \partial_{x_i}\partial_{x_j}a^{ij}(x,t)\rho(x,t) + \partial_{x_i}b^i(x,t)\rho(x,t) = 0.$$

FPE equation uses for analysis a macroscopic process but for a small subsystem.

We can formulate the singularly perturbed Cauchy problem for FPE in the form:

$$\varepsilon\partial_t\rho(x,t,\varepsilon) - \partial_{x_i}\partial_{x_j}a^{ij}(x,t)\rho(x,t,\varepsilon) + \partial_{x_i}b^i(x,t)\rho(x,t,\varepsilon) = 0,$$

$$\rho(x,0,\varepsilon) = \rho_0(x), \quad x \in \Omega, \quad \forall\rho_0(x) \in C_0^\infty(\Omega),$$

where $\varepsilon > 0$ is a small parameter.

If we assume $\varepsilon = 0$, we can get a degenerate Cauchy problem in the following form:

$$\partial_{x_i}\partial_{x_j}a^{ij}(x,t)\bar{\rho}(x,t) - \partial_{x_i}b^i(x,t)\bar{\rho}(x,t) = 0,$$

$$\bar{\rho}(x,0) = \rho_0(x), \quad x \in \Omega, \quad \forall\rho_0(x) \in C_0^\infty(\Omega),$$

where solutions $\bar{\rho}(x,t)$ are solutions of the degenerate problem and $\bar{\rho}$ may differ from solutions $\rho(x,t)$ significantly.

A large number of methods have been developed for the analytical and numerical study of FPE solutions [1]–[8]. Hyung Ju Hwang and Jinoh Kim [9], [10] study the initial–boundary value problem for the Vlasov–Poisson–Fokker–Planck equations in an interval with absorbing boundary conditions. They introduce the Deep Neural Network (DNN) approximated solutions to the kinetic Fokker–Planck equation in a bounded interval and study the large-time asymptotic behavior of the solutions and other physically relevant macroscopic quantities. Shu-Nan Li and Bing-Yang Cao [11] obtained solutions based on the fractional Fokker–Planck equation (FFPE) with a generic time- and length-dependence of an "effective thermal conductivity" (κ_{eff}), namely, $\kappa_{\text{eff}}L\alpha$ with L being the system length. They formulate the effective thermal conductivity in terms of entropy generation, which does not rely on the local-equilibrium hypothesis. Hrishikesh Patel and Bernie D. Shizgal [12] compare the Kappa distribution of space plasmas modelled with a particular Fokker–Planck equation for a two component system with the linear Fokker–Planck equation that has been used to study the Student t-distribution. Lucas Philip and Bernie D. Shizgal [13] consider the one-dimensional bistable Fokker–Planck equation with specific drift and diffusion coefficients so as to model protein folding. Yunfei Su and Lei Yao

[14] study the hydrodynamic limit for the inhomogeneous incompressible Fokker–Planck equations.

The development of the asymptotic analysis of singularly perturbed differential equations and systems of differential equations was made by A. N. Tikhonov [15], M. I. Vishik and L. A. Lyusternik [16], A. B. Vasil'eva [17], S. A. Lomov [18], V. A. Trenogin [19], J. L. Lions [20] and other researchers during the second half of the 20th century. There is a large number of recent works. O. Hawamdeh and A. Perjan [21] study an asymptotic expansions for linear symmetric hyperbolic systems with small parameter. Using the boundary layer functions method of Lyusternik–Vishik, A. Perjan [22] obtains the asymptotic expansions of the solutions to the Cauchy problem for the linear symmetric hyperbolic system as the small parameter $\varepsilon \to 0$. A. N. Gorban [23] investigates a model reduction in chemical dynamics with slow invariant manifolds and singular perturbations. Bor-Yann Chen, Liying Wu and Junming Hong [24] consider singular limits of reaction diffusion equations and geometric flows with discontinuous velocity.

In this paper we apply the results of the paper [21] and investigate the Cauchy problem for the singularly perturbed Tikhonov-type symmetric system of non-homogeneous constant coefficients linear parabolic partial differential equations (LPPDE system) with a small parameter. We use the asymptotic method for this Cauchy problem and construct expansions of solutions in the form of decomposition, which has regular and border-layer parts. The main result of this paper is a proof of a justification theorem of an asymptotic expansion for this Cauchy problem. Our method can be applied in a wide variety of cases for singularly perturbed Cauchy problems of Fokker–Planck equations.

2. Singularly perturbed Cauchy problem for LPPDE system

We consider the following singularly perturbed Cauchy problem (P_ϵ),

$$P_\epsilon u(x,t,\varepsilon) = f(x,t), \quad x \in \mathbf{R}^d, \quad t \geqslant 0, \tag{1}$$

$$u(x,0,\varepsilon) = u_0(x), \quad x \in \mathbf{R}^d, \tag{2}$$

where $\varepsilon > 0$ is a small parameter.

Thus, $P_\epsilon = P_0 + \varepsilon P_1$ is a parabolic operator, where $P_i = A_i\partial_t + B_i(\partial_x) + D_i$, $i = 0,1$,

$$B_i(\partial_x) = \sum_{p=1}^{d} B_{ip}\partial_{x_p} - \sum_{p,q=1}^{d} C_{ipq}\partial_{x_p}\partial_{x_q},$$

$B_{ip} = (b_{st}^{ip})_{s,t=1}^{n}$, $C_{ipq} = (c_{st}^{ipq})_{s,t=1}^{n}$, $D_i = (d_{st}^{i})_{s,t=1}^{n}$ are real constants of symmetric $n \times n$ matrices and $b_{st}^{ip} \geqslant 0$, $c_{st}^{ipq} \geqslant 0$, $d_{st}^{i} \geqslant 0$ $(\forall s,t = 1,\dots,n)$, $d \geqslant 1$, $u(x,0,\varepsilon) : \mathbf{R}^d \times [0,\infty) \times (0,\infty) \to \mathbf{R}^n$, $f(x,t) : \mathbf{R}^d \times [0,\infty) \to \mathbf{R}^n$, $f(x,t) \in C^1$,

$$A_0 = \begin{pmatrix} I_m & 0 \\ 0 & 0 \end{pmatrix}, \quad A_1 = \begin{pmatrix} 0 & 0 \\ 0 & I_{n-m} \end{pmatrix}, \quad 0 \leqslant m \leqslant n,$$

where I_k is an identity matrix and

$$A = A_0 + \varepsilon A_1, \quad B(\partial_x) = B_0(\partial_x) + \varepsilon B_1(\partial_x), \quad D = D_0 + \varepsilon D_1,$$
$$L_i(\partial_x) = B_i(\partial_x) + D_i, \quad i = 0, 1, \quad \partial_x = (\partial/\partial_{x_1}, \dots, \partial/\partial_{x_d}).$$

The special forms of matrices A_0 and A_1 determine the natural representations of matrices B_i, D_i by blocks in the forms:

$$B_i(\partial_x) = \begin{pmatrix} B_{i1}(\partial_x) & B_{i2}(\partial_x) \\ B_{i2}^*(\partial_x) & B_{i3}(\partial_x) \end{pmatrix}, \quad D_i = \begin{pmatrix} D_{i1} & D_{i2} \\ D_{i2}^* & D_{i3} \end{pmatrix}, \quad i = 0, 1,$$

where $B_{i1}(\partial_x)$, $D_{i1} \in M^{m\times m}(\mathbf{R})$, $B_{i2}(\partial_x)$, $D_{i2} \in M^{m\times(n-m)}(\mathbf{R})$, $B_{i3}(\partial_x)$, $D_{i3} \in M^{(n-m)\times(n-m)}(\mathbf{R})$, and $*$ means transposition, and

$$B_{ij}(\partial_x) = \sum_{p=1}^{d} B_p^{ij} \partial_{x_p} - \sum_{p,q=1}^{d} C_{pq}^{ij} \partial_{x_p} \partial_{x_q}, \quad i = 0, 1,\ j = 1, 2, 3,$$

$$B_p^{01} = (b_{st}^{0p})_{s,t=\overline{1,m}}, \quad C_{pq}^{01} = (c_{st}^{0pq})_{s,t=\overline{1,m}},$$
$$B_p^{02} = (b_{st}^{0p})_{s=\overline{1,m},t=\overline{m+1,n}}, \quad C_{pq}^{02} = (c_{st}^{0pq})_{s=\overline{1,m},t=\overline{m+1,n}},$$
$$B_p^{03} = (b_{st}^{0p})_{s,t=\overline{m+1,n}}, \quad C_{pq}^{02} = (c_{st}^{0pq})_{s,t=\overline{m+1,n}}.$$

The aim of our work is to construct the asymptotic solution $u(\varepsilon, x, t)$ for (P_ε) with a small parameter $\varepsilon \to 0$.

Thus, the investigation of the solution $u(\varepsilon, x, t)$ depends on the structure of the operator P_ε. The norm, which determines the convergence of the perturbed system solution, is also very important.

We denote the usual Sobolev spaces by H^s with the scalar product in the form:

$$(u, v)_s = \int_{\mathbf{R}^d} (1 + \xi^2)^s \hat{u}(\xi) \bar{\hat{v}}(\xi)\, d\xi,$$

where $s \in \mathbf{R}$, $\hat{u}(\xi) = F[u]$ ($\xi \in \mathbf{R}^d$) and $F^{-1}[u]$ are the direct and the inverse Fourier transforms of the function u in S'. Let $H_d^s = (H^s)^d$ be a notation of the Hilbert space, which is associated with the scalar product

$$(f_1, f_2)_{s,d} = \sum_{j=1}^{d} (f_{1j}, f_{2j})_s, \quad f_i = (f_{i1}, \dots, f_{id}), \quad i = 1, 2,$$

and with the norm $\| \cdot \|_{s,d}$, which is generated by this scalar product.

Let $D'((a,b),X)$ be a space of vectorial distributions on (a,b) with values in Banach space X. We can set

$$W^{k,p}(a,b;X) = \{u \in D'((a,b);X);\ u^{(j)} \in L^p(a,b;X),\ j = 0,1,\dots,k\},$$

for $k \in \mathbb{N}^*$ and $1 \leqslant p \leqslant \infty$, where $u^{(j)}$ is the distributional derivative of order j and $W^{0,p}(a,b;X) = L^p(a,b;X)$ for $k = 0$.

We denote operator $L_{ij}(\partial_x)$ in the form:

$$L_{ij}(\partial_x) = B_{ij}(\partial_x) + D_{ij},$$

and

$$F = \mathrm{col}(f,g), \quad U_0 = \mathrm{col}(u_0,u_1),$$

where $f, u_0 \in M^{m\times 1}(\mathbf{R})$, $g, u_1 \in M^{(n-m)\times 1}(\mathbf{R})$.

We assume that

H1: B_{ip}, C_{ipq}, D_i, $i = 0,1$, $p,q = \overline{1,d}$ are real symmetric matrices;

H2: $(D\zeta,\zeta)_{\mathbf{R}^n} \geqslant (D_{03}\eta,\eta)_{\mathbf{R}^{n-m}} \geqslant q_0|\eta|^2$, with $q_0 > 0$; for all $\zeta \in \mathbf{R}^n$ and $\eta \in \mathbf{R}^{n-m}$.

Thus, the operator (P_ε) is a symmetric parabolic system (**H1**) and the operator (P_0) is an elliptic-parabolic system in case: *det* $B_{03} \neq 0$ and $B_{02} = 0$.

3. Formal asymptotic expansions of the singularly perturbed Cauchy problem (P_ϵ)

We construct the formal asymptotic expansions of the solutions $u(\varepsilon,x,t)$ for the Cauchy problem (P_ε) on the positive powers of the small parameter ε in this section.

We can use the following asymptotic expansion of the solution $u(\varepsilon,x,t)$ for the problem (P_ε) according to the method of Lyusternik–Vishik [16]:

$$u(\varepsilon,x,t) = V(x,t,\varepsilon) + Z(x,\tau) = \sum_{k=0}^{N} \varepsilon^k (V_k(x,t) + Z_k(x,\tau)) + R_N(\varepsilon,x,t), \quad (3)$$

where $\tau = t/\varepsilon$, and $Z(x,\tau) = Z_0(x,\tau) + \dots + \varepsilon^N Z_N(x,\tau)$ is the boundary layer function, which describes the singular behavior of the solution $u(\varepsilon,x,t)$ within a neighborhood of the set $\{(x,0),\, x \in \mathbf{R}^d\}$, which is the boundary layer.

The function $V(x,t) = V_0(x,t) + \dots + \varepsilon^N V_N(x,t)$ is the regular part of expansion (3).

We assume that the function $Z(x,\tau)$ is small for large τ, i.e. $Z \to 0$ as $\tau \to \infty$. There is the solutions behavior $u(\varepsilon,x,t) \not\to u(0,x,t)$ of the singularly perturbed Cauchy problem (P_ϵ), when $\varepsilon \to 0$ within the boundary layer, then the function $Z(x,\tau)$ has to be reduced for the discrepancy elimination of the solutions $u(\varepsilon,x,0)$ and $u(0,x,0)$.

We can substitute expansion (3) into (1) formally and identify the coefficients of the same powers of ε, which contain the same variables.

Then we can get the following equations:

$$P_0 V_k = F_k(x,t), \quad x \in \mathbf{R}^d, \quad t > 0, \tag{4}$$

where

$$\begin{gathered} F_0 = f(x,t), \quad F_k = -P_1 V_{k-1}, \quad k = 1,\dots,N, \\ A_0 \partial_\tau Z_k = F_k(x,\tau), \quad k = 0,1,\dots,N, \\ A_1(L_0 Z_N + L_1 Z_{N-1} + \partial_\tau Z_N) = 0, \quad x \in \mathbf{R}^d, \quad \tau > 0, \\ F_0 = 0, \quad F_1 = -L_0 Z_0 - A_1 \partial_\tau Z_0, \\ F_k = -L_0 Z_{k-1} - L_1 Z_{k-2} - A_1 \partial_\tau Z_{k-1}, \quad k = 2,\dots,N, \end{gathered} \tag{5}$$

$$\begin{gathered} (P_0 + \varepsilon P_1) R_N = F(x,t,\varepsilon), \quad x \in \mathbf{R}^d, \quad t > 0, \\ F = -\varepsilon^{N+1}(P_1 V_N + L_1 Z_N) - \varepsilon^N A_0 (L_0 Z_N + L_1 Z_{N-1}). \end{gathered} \tag{6}$$

We can substitute (3) into initial condition (2)

$$R_N(\varepsilon, x, 0) = 0, \quad x \in \mathbf{R}^d, \tag{7}$$

$$V_0(x,0) + Z_0(x,0) = U_0(x), \quad x \in \mathbf{R}^d, \tag{8}$$

$$V_k(x,0) + Z_k(x,0) = 0,\ x \in \mathbf{R}^d, \quad k = 1,\dots,N. \tag{9}$$

We can use the following notation for convenience

$$Z_k = \begin{pmatrix} X_k \\ Y_k \end{pmatrix}, \quad V_k = \begin{pmatrix} v_k \\ w_k \end{pmatrix}, \quad F_k = \begin{pmatrix} f_k \\ d_k \end{pmatrix}, \quad F_k = \begin{pmatrix} F_{k1} \\ F_{k2} \end{pmatrix}, \tag{10}$$

where $X_k, v_k, f_k, F_{k1} \in M^{m\times 1}(\mathbf{R})$, $Y_k, w_k, g_k, F_{k2} \in M^{(n-m)\times 1}(\mathbf{R})$.

We can use (5), (8), and (9) for X_k and Y_k so that

$$\partial_\tau X_k = F_{k1}, \quad X_k \to 0, \quad \tau \to +\infty, \tag{11}$$

and

$$\begin{gathered} \partial_\tau Y_k + L_{03} Y_k = F_{k2}(x,\tau), \quad x \in \mathbf{R}^d, \quad \tau > 0, \\ Y_0(x,0) = u_1(x) - w_0(x,0), \quad x \in \mathbf{R}^d, \\ Y_k(x,0) = -w_k(x,0), \quad k = 1,\dots,N, \quad x \in \mathbf{R}^d, \end{gathered} \tag{12}$$

where

$$\begin{gathered} F_{01} = 0, \quad F_{11} = -L_{01} X_0 - L_{02} Y_0, \\ F_{k1} = -L_{01} X_{k-1} - L_{02} Y_{k-1} - L_{11} X_{k-2} - L_{12} Y_{k-2}, \quad k = 2,\dots,N, \\ F_{02} = -L^*_{02} X_0, \quad F_{k2} = -L^*_{02} X_k - L_{13} Y_{k-1} - L^*_{12} X_{k-1}, \quad k = 1,\dots,N \\ L^*_{ij}(\xi) = B^*_{ij}(\xi) + D^*_{ij}, \quad i = 0,1, \quad j = 1,2,3. \end{gathered}$$

Similarly, we can obtain the problems for v_k and w_k from (4) and (8), (9).

$$\begin{cases} \partial_t v_k + L_{01} v_k + L_{02} w_k = f_k(x,t), \quad k = 0,1,\dots,N, \\ L_{02}^* v_k + L_{03} w_k = g_k(x,t), \quad x \in \mathbf{R}^d, \quad k = 0,1,\dots,N, \quad t > 0, \\ v_0(x,0) = u_0(x) - X_0(x,0), \\ v_k(x,0) = -X_k(x,0), \quad k = 1,\dots,N, \quad x \in \mathbf{R}^d. \end{cases} \tag{13}$$

Thus, we have the problems for determining the functions X_k, Y_k, v_k, w_k and R_N.

4. Justifying asymptotic expansions of the singularly perturbed Cauchy problem (P_ϵ)

We investigate the validity of the expansion (3) in the following sections. We can consider the problem (13) in the next form

$$\begin{cases} \partial_t v + L_{01} v + L_{02} w = f(x,t), \\ L_{02}^* v + L_{03} w = g(x,t), \quad x \in \mathbf{R}^d, \quad t > 0, \\ v(x,0) = h(x), \quad x \in \mathbf{R}^d, \end{cases} \tag{14}$$

$$L_{0j} = B_{0j}(\partial_x) + D_{0j} = \sum_{p=1}^{d} B_p^{0j} \partial_{x_p} - \sum_{p,q=1}^{d} C_{pq}^{0j} \partial_{x_p} \partial_{x_q} + D_{0j}, \quad j = 1,2,3.$$

We use the following problem for the solvability and regularity justifications of the problem (14)

$$\begin{cases} \partial_t \hat{v}(\xi) + (D_{01} + i|\xi|\hat{B}_{01}(\xi))\hat{v}(\xi) + (D_{02} + i|\xi|\hat{B}_{02}(\xi))\hat{w}(\xi) = \hat{f}(\xi,t), \\ (D_{02}^* + i|\xi|\hat{B}_{02}^*(\xi))\hat{v}(\xi) + (D_{03} + i|\xi|\hat{B}_{03}(\xi))\hat{w}(\xi) = \hat{g}(\xi,t), \\ \hat{v}(\xi,0) = \hat{h}(\xi), \end{cases}$$

$$\hat{B}_{ij}(\xi) = \sum_{p=1}^{d} B_p^{0j}(\xi_p/|\xi|) - i|\xi| \sum_{p,q=1}^{d} C_{pq}^{0j}(\xi_p \xi_q/|\xi|^2), \tag{15}$$

where $i = 0,1$, $j = 1,2,3$, $\xi \in \mathbf{R}^d$.

We prove the following lemmas.

Lemma 1. *The matrix $D_{03} + i|\xi|\hat{B}_{03}(\xi)$ is invertible for $\xi \in \mathbf{R}^d$ under the assumptions (**H1**), (**H2**) and the function $\xi \to (D_{03} + i|\xi|\hat{B}_{03}(\xi))^{-1}$ is bounded on $\mathbf{R}^d$.*

Proof. We can use the method of the simultaneous reduction of two matrices to the diagonal form for proving this lemma and we assume that

$D_{03}^* = D_{03}$ and $D_{03} = (d_{st}^0)_{s,t=\overline{n-m,n}}$, $d_{st}^0 \geqslant 0$ $(s,t=\overline{n-m,n})$. There is an orthogonal matrix $T_1 \in M^{n-m}(\mathbf{R})$, $T_1^* T_1 = I_{n-m}$, which

$$T_1^* D_{03} T_1 = \Lambda_0^2 = \mathrm{diag}(\lambda_1, \dots, \lambda_{n-m}),$$

where $\lambda_k > 0$, $k = 1, \dots, n-m$ are the eigenvalues of matrix D_{03}.

We can use the transformation of the matrix $\widehat{B}_{03}(\xi)$ in the form:

$$C(\xi) = \Lambda_0^{-1} T_1^* \widehat{B}_{03}(\xi) T_1 \Lambda_0^{-1}.$$

As the matrix $C(\xi)$ is a real symmetric, then there exists an orthogonal matrix $T_2(\xi) \in M(\mathbf{R}^{n-m})$, such that

$$T_2^* C(\xi) T_2 = \Lambda(\xi) = \mathrm{diag}(\mu_1(\xi), \dots, \mu_{n-m}(\xi)),$$

where $\mu_1(\xi), \dots, \mu_{n-m}(\xi)$ are real eigenvalues of matrix $C(\xi)$. Thus, we have the transformations of this type:

$$T^*(\xi) D_{03} T(\xi) = I_{n-m}, \quad T^*(\xi) \widehat{B}_{03}(\xi) T(\xi) = \Lambda(\xi), \tag{16}$$

where $T(\xi) = T_1 \Lambda_0^{-1} T_2(\xi)$. We can use (16) so that

$$D_{03} + i|\xi| \widehat{B}_{03}(\xi) = T^{*^{-1}}(\xi)(I_{n-m} + i|\xi|\Lambda(\xi)) T^{-1}(\xi).$$

It means that the matrix $D_{03} + i|\xi|\widehat{B}_{03}(\xi)$ is invertible and we have

$$(D_{03} + i|\xi|\widehat{B}_{03}(\xi))^{-1} = T(\xi)\Lambda_1(\xi)(I_{n-m} - i|\xi|\Lambda(\xi)) T^*(\xi), \tag{17}$$

where

$$\Lambda_1(\xi) = \mathrm{diag}((1 + |\xi|^2 \mu_1^2)^{-1}, \dots, (1 + |\xi|^2 \mu_{n-m}^2)^{-1}).$$

The orthogonality of the matrix $T_2(\xi)$ implies the boundedness of the function $\xi \to T(\xi)$ on $\mathbf{R}^d$.

The boundedness of the matrix $(D_{03} + i|\xi|\widehat{B}_{03}(\xi))^{-1}$ follows from (17). Lemma 1 is proved. □

We can obtain the solution of the problem (15) from Lemma 1

$$\begin{cases} \dfrac{d}{dt}\widehat{v}(\xi,t) + K(\xi)\widehat{v}(\xi,t) = H(\xi,t), \\ \widehat{v}(\xi,0) = \widehat{h}(\xi), \end{cases} \tag{18}$$

where

$$\widehat{w}(\xi,t) = (D_{03} + i|\xi|\widehat{B}_{03}(\xi))^{-1}(\widehat{g}(\xi,t) - (D_{02}^* + i|\xi|\widehat{B}_{02}^*(\xi))\widehat{v}(\xi,t)), \tag{19}$$

$$K(\xi) = D_{01} + i|\xi|\widehat{B}_{01}(\xi) - (D_{02} + i|\xi|\widehat{B}_{02}(\xi))(D_{03} + \\ + i|\xi|\widehat{B}_{03}(\xi))^{-1}(D_{02}^* + i|\xi|\widehat{B}_{02}^*(\xi)), \tag{20}$$

$$H(\xi,t) = \hat{f}(\xi,t) - (D_{02} + i|\xi|\hat{B}_{02}(\xi))(D_{03} + i|\xi|\hat{B}_{03}(\xi))^{-1}\hat{g}(\xi,t).$$

Lemma 2. *The matrix $K(\xi)$ can be represented in the form*

$$K(\xi) = K_0(\xi) + i|\xi|K_1(\xi) + |\xi|^2 K_2(\xi), \quad \xi \in \mathbf{R}^d, \tag{21}$$

*under the assumptions (**H1**), (**H2**), where the functions $\xi \to K_j(\xi)$, $j = 0,1,2$ are bounded on $\mathbf{R}^d$ and K_1, K_2 are real symmetric for $K_2 \geqslant 0$.*

Proof. Let us substitute (17) into (20). We can obtain the representation (21), where

$$K_0(\xi) = G_{01} - G_{02}T^*\Lambda_1 T^* G_{02}^* - |\xi|^2(G_{02}T\Lambda_1\Lambda T^* b_{02}^* + b_{02}T\Lambda_1\Lambda T^* G_{02}^*),$$

$$K_1(\xi) = b_{01} + G_{02}T\Lambda_1\Lambda T^* G_{02}^* - G_{02}T\Lambda_1 T^* b_{02}^* - \\ - b_{02}T\Lambda_1 T^* G_{02}^* - |\xi|^2 b_{02}T\Lambda_1\Lambda T^* b_{02}^*,$$

$$K_2(\xi) = b_{02}T\Lambda_1 T^* b_{02}^*.$$

Accordingly, $K_j(\xi)$, $j = 0,1,2$ are bounded on $\mathbf{R}^d$ and $K_1^* = K_1$, $K_2^* = K_2$. It remains to prove that $K_2 \geqslant 0$. Let us denote the eigenvalues of the real symmetric matrix A as $\lambda_j(A)$, $j = 1,\dots,m$, where $\lambda_1 \leqslant \lambda_2 \leqslant \dots \leqslant \lambda_m$.

We can use Ostrowski's theorem so that

$$\lambda_j(K_2(\xi)) = \lambda_j(b_{02}T\Lambda_1 T^* b_{02}^*) = \theta_j \lambda_j(\Lambda_1) \geqslant 0,$$

where $0 \leqslant \lambda_1(b_{02}TT^*b_{02}^*) \leqslant \theta_j \leqslant \lambda_m(b_{02}TT^*b_{02}^*)$. It means that $K_2 \geqslant 0$. Therefore, Lemma 2 is proved. □

We can prove the following proposition.

Proposition 1. Let the assumptions (**H1**), (**H2**) be fulfilled and $l \in \mathbb{N}^*$. If the conditions $h \in H_m^{s+2l+1}$, $F = \mathrm{col}(f,g) \in W^{l,1}(0,T;H_n^{s+2})$ are true, then there exists a unique strong solution $V = \mathrm{col}(v,w) \in W^{l,\infty}(0,T;H_n^s)$ of the problem (14) and

$$\|V\|_{W^{l,\infty}(0,T;H_n^s)} \leqslant C(T)\left(\|h\|_{s+2l+1,m} + \|F\|_{W^{l,1}(0,T;H_n^{s+2})}\right). \tag{22}$$

Proof. Consider the Cauchy problem

$$\begin{cases} \frac{d}{dt}\hat{v}(t) + K(\xi)\hat{v}(t) = 0, \\ \hat{v}(0) = \hat{h}, \quad 0 < t < T, \end{cases} \tag{23}$$

in the Hilbert space $H = \{f = (f_1,\dots,f_m);\ (1+|\xi|^2)^{\frac{s}{2}} f_k(\xi) \in L^2(\mathbf{R}^d),\ k = 1,\dots,m\}$, equipped with the scalar product $(f,g)_H = \int_{\mathbf{R}^d} (1+$

$|\xi|^2)^s(f,\bar{g})_{\mathbf{R}^m}\,d\xi$. We can use the representation (21) and demonstrate that the operator $-K(\xi): H \to H$ satisfies the conditions

$$\mathrm{Re}(-Kf,f)_H \leqslant \omega(f,f)_H,\ \mathrm{Re}(-\bar{K}^*f,f)_H \leqslant \omega(f,f)_H, \quad f \in H,$$

where $\omega = sup_{\xi\in\mathbf{R}^d}\|K_0(\xi)\|_{\mathbf{R}^m\to\mathbf{R}^m} + \delta$ with a positive parameter $\delta > 0$. This means that the operator $-(K+\omega I)$ is maximal dissipative on H.

The Cauchy problem (23) generates a C_0 semigroup of operators $\{\hat{T}(t),\ t \geqslant 0\}$ on H [21]. Thus, we have the next estimation $\|\hat{v}(\cdot,t)\|_H \leqslant e^{\omega t}\|h\|_H$ for any $h \in H$, i.e. $\|\hat{T}(t)\| \leqslant e^{\omega t}$, where

$$\frac{d}{dt}\|\hat{v}(\cdot,t)\|_H^2 \leqslant -(K_0\hat{v}(\cdot,t),\hat{v}(\cdot,t))_H - (\hat{v}(\cdot,t),K_0\hat{v}(\cdot,t))_H \leqslant 2\omega\|\hat{v}(\cdot,t)\|_H^2.$$

Using Parseval's equality, we can get that the Cauchy problem ($F[\check{K}v] = K(\xi)\hat{v}$)

$$\begin{cases} \dfrac{d}{dt}v(t) + \check{K}v(t) = 0, \\ v(0) = v_0, \quad 0 < t < T, \end{cases} \tag{24}$$

where the operators $\{T(t), t \geqslant 0\}$ on H_m^s generates the semigroup C_0, where $v(\cdot,t) = T(t)v_0$, $\|T(t)\| \leqslant e^{\omega t}$. Thus, we can solve the Cauchy problem

$$\begin{cases} \dfrac{d}{dt}z(t) + (\check{K}+\omega I)z(t) = f(t)e^{\omega t}, \\ z(0) = y_0, \quad 0 < t < T, \end{cases} \tag{25}$$

where the semigroup C_0 has the representation in the form $T_0(t) = T(t)e^{-\omega t}$.

Hence, there exists a unique mild solution of this problem $z \in C([0,T]; H_m^s)$ for every $y_0 \in H_m^s$, $f \in L^1(0,T;H_m^s)$ [21], and

$$z(t) = T_0(t)y_0 + \int_0^t T_0(t-s)f(s)e^{\omega s}ds,$$

$$\|z\|_{C([0,T];H_m^s)} \leqslant \|y_0\|_{s,m} + \|f\|_{L^1(0,T;H_m^s)}e^{\omega T}.$$

Moreover, if the next $y_0 \in H_m^{s+2l}$, $f \in W^{l,1}(0,T;H_m^s)$ and $l \in \mathbb{N}^*$ are true, then z is a strong solution of the problem (25), $z \in W^{l,\infty}(0,T;H_m^s)$ and

$$\|z\|_{W^{l,\infty}(0,T;H_m^s)} \leqslant C(T)(\|y_0\|_{s+2l,m} + \|f\|_{W^{l,1}(0,T;H_m^s)}).$$

We can note that the solution y of the Cauchy problem

$$\begin{cases} \frac{d}{dt}y(t) + \check{K}y(t) = f, \\ y(0) = y_0, \quad 0 < t < T, \end{cases} \tag{26}$$

and the solution z of the problem (25) are connected with the equality $y(t) = e^{-\omega t} z(t)$.

Consequently, we have the same for y_0, f and $l \in N^*$ so that

$$\|y\|_{W^{l,\infty}(0,T;H^s_m)} \leqslant C(T)(\|y_0\|_{s+2l,m} + \|f\|_{W^{l,1}(0,T;H^s_m)}).$$

Using (18), the last estimation and the boundedness of the matrix $(G_{03} + i|\xi|b(\xi))^{-1}$, we can obtain the next estimation

$$\|v\|_{W^{l,\infty}(0,T;H^s_m)} \leqslant \\ \leqslant C(T)(\|h\|_{s+2l,m} + \|f\|_{W^{l,1}(0,T;H^s_m)} + \|g\|_{W^{l,1}(0,T;H^{s+1}_{n-m})}). \quad (27)$$

We can get the estimation from (19) and (27) in the form:

$$\|w\|_{W^{l,\infty}(0,T;H^s_m)} \leqslant \\ \leqslant C(T)\left(\|h\|_{s+2l+1,m} + \|f\|_{W^{l,1}(0,T;H^{s+1}_m)} + \|g\|_{W^{l,1}(0,T;H^{s+2}_{n-m})}\right). \quad (28)$$

Thus, the estimations (27) and (28) imply the estimation (23). Proposition 1 is proved. □

Let us consider the next Cauchy problem

$$\begin{cases} \partial_\tau Y + L_{03} Y = F(x,\tau),\ x \in \mathbf{R}^d, \quad \tau > 0, \\ Y(x,0) = y_0(x), \quad x \in \mathbf{R}^d. \end{cases} \quad (29)$$

Proposition 2. Let the assumptions (**H1**), (**H2**) be fulfilled and $l \in \mathbb{N}^*$. If the conditions $y_0 \in H^{s+l}_{n-m}$, $F \in W^{l,1}_{\text{loc}}(0,\infty; H^s_{n-m})$ are true, then there exists a unique strong solution $Y \in W^{l,\infty}_{\text{loc}}(0,\infty; H^s_{n-m})$ of the problem (29) and the inequality is satisfied for this solution

$$\|\partial^l_\tau Y(\cdot,\tau)\|_{s,n-m} \leqslant C e^{-q_0 \tau}(\|y_0\|_{s+l,n-m} + \\ + \sum_{\nu=0}^{l-1} \|\partial^\nu_\tau F(\cdot,0)\|_{s+l-\nu-1,n-m} + \int_0^\tau e^{q_0\theta} \|\partial^l_\tau F(\cdot,\theta)\|_{s,n-m}\, d\theta). \quad (30)$$

Proof. The operator $-L_{03}(\partial_x)$ is a dissipative under the assumptions (**H1**), (**H2**) and it generates the C_0 semigroup of the contractions $S(\tau)$ on H^s_{n-m}. Thus, there exists a unique mild solution $Y \in C([0,\infty); H^s_{n-m})$ of the Cauchy problem (29). Hence, we can obtain the estimation $\|S(\tau)\| \leqslant e^{-q_0\tau}$, $\tau \geqslant 0$, which with the next equality

$$Y(\cdot,\tau) = S(\tau) y_0 + \int_0^\tau S(\theta) F(\cdot, \tau - \theta)\, d\theta$$

gives the estimation (30) in the case $l = 0$. We can obtain the estimation (30) by differentiating to τ the equation (29) in the case $l \geqslant 1$. Proposition 2 is proved. □

Using these propositions, we can determine the functions V_k and Z_k. Hence, it follows from (11) for $k = 0$ that $X_0 = 0$. We can find the main regular term $V_0 = \mathrm{col}(v_0, w_0)$ of the expansion (3) from (13) and Proposition 1. Instantly, we have the following:

$$w_0(x, 0) = F^{-1}[(G_{03} + i|\xi|b_{03}(\xi))^{-1}(\hat{g}(\xi, 0) - (G^*_{02} + i|\xi|b^*_{02}(\xi))\hat{u}_0(\xi))].$$

Lemma 1 and the Parseval equality permit us to obtain the next estimation

$$\|w_0(\cdot, 0)\|_{s,n-m} \leqslant C(\|g(\cdot, 0)\|_{s,n-m} + \|u_0\|_{s+1,m}) \leqslant \\ \leqslant C(\|U_0\|_{s+1,n} + \|F(\cdot, 0)\|_{s,n}). \quad (31)$$

Proposition 2 permits us to define the function Y_0 as a solution of Cauchy problem (12). Moreover, we can obtain the next inequality from (30) and (31)

$$\|\partial^l_\tau Y_0(\cdot, \tau)\|_{s,n-m} \leqslant Ce^{-q_0\tau}(\|U_0\|_{s+l+1,n} + \|F(\cdot, 0)\|_{s+l,n}). \quad (32)$$

Thus, we can find the main singular term $Z_0 = \mathrm{col}(0, Y_0)$ of the expansion (3).

Let us obtain the next terms of this expansion. Let us suppose that the terms $V_0, \dots, V_{k-1}$ and $Z_0, \dots, Z_{k-1}$ are already found. We can obtain the terms V_k and Z_k and show that the next estimations

$$\|V_k\|_{W^{l,\infty}(0,T;H^s_n)} \leqslant C(T)(\|U_0\|_{s+2l+3k+1,n} + \\ + \|F(\cdot, 0)\|_{s+2l+3k-2,n} + \|F\|_{W^{l,1}(0,T;H^{s+3k+2}_n)}), \quad (33)$$

and

$$\|\partial^l_\tau Z_k(\cdot, \tau)\|_{s,n} \leqslant Ce^{-q_0\tau}(1 + \tau^k)\left(\|U_0\|_{s+l+k+1,n} + \|F(\cdot, 0)\|_{s+l+k,n}\right) \quad (34)$$

are true, if we suppose that such estimations are true for previous terms. We can note that the estimations (33), (34) for V_0 and Z_0 follow from (22) and (32).

At first, if we solve the problem (11), we can get

$$X_k(\cdot, \tau) = -\int_\tau^\infty F_{k1}(\cdot, \theta)\, d\theta,$$

where the integral exists due to the estimation (34) for Z_{k-1}. Using (34) for Z_{k-1} and for Z_{k-2}, we obtain the next estimation:

$$\|\partial^l_\tau X_k(\cdot, \tau)\|_{s,m} = \|\partial^{l-1}_\tau F_{k1}(\cdot, \tau)\|_{s,m} \leqslant \\ \leqslant C(\|\partial^{l-1}_\tau Z_{k-1}(\cdot, \tau)\|_{s+1,n} + \|\partial^{l-1}_\tau Z_{k-2}(\cdot, \tau)\|_{s+1,n}) \leqslant \\ \leqslant Ce^{-q_0\tau}(1 + \tau^{k-1})(\|U_0\|_{s+l+k,n} + \|F(\cdot, 0)\|_{s+l+k-1,n}), \quad (35)$$

for $l \geqslant 1$. Similarly, we can get the estimation (35) in the case $l = 0$.

Using Proposition 1 and $v_k(\cdot, 0) = -X_k(\cdot, 0)$, we can solve the problem (13) and find the functions V_k.

Using the next estimation

$$\|V_k\|_{W^{l,\infty}(0,T;H_n^s)} \leqslant C(T)(\|X_k(\cdot,0)\|_{s+2l+1,m} + \|V_{k-1}\|_{W^{l,\infty}(0,T;H_n^{s+3})}),$$

and also (22), (33) for V_{k-1} and (35) for X_k, we can find the estimation (33) for V_k.

Instantly, we can obtain the next equality

$$w_k(x,0) = F^{-1}[(D_{03} + i|\xi|\hat{B}_{03}(\xi))^{-1}(\hat{g}_k(\xi,0) - (D_{02}^* + i|\xi|\hat{B}_{02}^*(\xi))\hat{X}_k(\xi,0))]$$

and establish the estimation

$$\begin{aligned} \|w_k(\cdot,0)\|_{s,n-m} &\leqslant C(\|g_k(\cdot,0)\|_{s,n-m} + \|X_k(\cdot,0)\|_{s+1,m}) \leqslant \\ &\leqslant C(\|X_{k-1}(\cdot,0)\|_{s+1,m} + \|X_k(\cdot,0)\|_{s+1,m} + \|w_{k-1}(\cdot,0)\|_{s+1,n-m}) \leqslant \\ &\leqslant C(\|U_0\|_{s+k+1,n} + \|F(\cdot,0)\|_{s+k,n}). \end{aligned} \tag{36}$$

Using (34) for Z_{k-1} and (35) for X_k, we can obtain the next unequality

$$\begin{aligned} \|\partial_\tau^l F_{k2}(\cdot,\tau)\|_{s,n-m} &\leqslant C(\|\partial_\tau^l X_k(\cdot,\tau)\|_{s+1,m} + \|\partial_\tau^l Z_{k-1}(\cdot,\tau)\|_{s+1,n}) \leqslant \\ &\leqslant Ce^{-q_0\tau}(1+\tau^{k-1})(\|U_0\|_{s+l+k+1,n} + \|F(\cdot,0)\|_{s+l+k,n}). \end{aligned} \tag{37}$$

We can find the next estimation from (30), (36) and (37)

$$\begin{aligned} \|\partial_\tau^l Y_k(\cdot,\tau)\|_{s,n-m} &\leqslant Ce^{-q_0\tau}(\|w_k(\cdot,0)\|_{s+l,n-m} + \\ &+ \sum_{\nu=0}^{l-1} \|\partial_\tau^\nu F_{k2}(\cdot,0)\|_{s+l-\nu-1,n-m} + \int_0^\tau e^{q_0\theta}\|\partial_\tau^l F_{k2}(\cdot,\theta)\|_{s,n-m}\,d\theta) \leqslant \\ &\leqslant Ce^{-q_0\tau}(1+\tau^k)(\|U_0\|_{s+l+k+1,n} + \|F(\cdot,0)\|_{s+l+k,n}). \end{aligned} \tag{38}$$

The estimations (35) and (38) imply the estimation (34) for Z_k.

We can prove the main result of our work.

Theorem 1. *Let us suppose that B and G satisfy conditions (**H1**), (**H2**) and $0 \leqslant l < N+1$. If the conditions $U_0 \in H_n^{s+2l+3(N+1)}$, $F \in W^{l+1,1}(0,T;H_n^{s+2l+3(N+1)})$ are true, then there exists a unique strong solution $U \in W^{l,\infty}(0,T;H_n^s)$ of the problem (P_ε). The expansion (3) is true for this solution, where V_k and Z_k are determined by problems (13), (11), (12) respectively and they satisfy the estimations (33), (34). The estimation*

$$\|R_{N1}\|^2_{W^{l,\infty}(0,T;H_m^s)} + \varepsilon^{1/2}\|R_{N2}\|^2_{W^{l,\infty}(0,T;H_{n-m}^s)} \leqslant C(T)\varepsilon^{N+1-l} \tag{39}$$

is true with $C(T)$ depending on T, $\|U_0\|_{s+2l+3(N+1),n}$, $\|F\|_{W^{l+1,1}(0,T;H_n^{s+2l+3(N+1)})}$ and q_0 for the remainder term $R_N = \mathrm{col}(R_{N1}, R_{N2})$. In particular, if we assume $N = 0$, then there is the next estimation

$$\|U - V_0 - Z_0\|_{C([0,T];H_n^s)} \leqslant C(T)\varepsilon^{1/4}.$$

Proof. Using the properties of the C_0 semigroup of operators, we can obtain the solvability of the problem (P_ε). Indeed, the operator $-(B(\partial_x)+D)$ is closed and dissipative on H_n^s. This operator generates the C_0 semigroup of contractions on H_n^s, which solves the problem (P_ε). Moreover, the conditions $U_0 \in H_n^{s+l}$, $F \in W^{l,1}(0,T;H_n^s)$, $\partial_t^\nu F(\cdot,0) \in H_n^{s+l-\nu-1}$, $\nu = 0,\dots,l-1$, $l \geqslant 1$ imply the regularity of the solution $U \in W^{l,\infty}(0,T;H_n^s)$. Using the method from [21], we can prove the estimation (39). Furthermore, all constants depend on the norms, which are indicated in the Theorem 1, and they are represented by $C(T)$. Let us denote the next relations $R_l = \partial_t^l R_N$, $R_{li} = \partial_t^l R_{Ni}$, $i = 1, 2$. We can find that $(BR_l, R_l)_{s,n}$ is a pure imaginary value from the condition (**H1**). Consequently, we can get the next equation

$$\frac{d}{dt}(AR_l(\cdot,t),R_l(\cdot,t))_{s,n} + 2(GR_l(\cdot,t),R_l(\cdot,t))_{s,n} = 2Re(\partial_t^l F(\cdot,t),R_l(\cdot,t))_{s,n}.$$

Using the assumption $(H2)$, we can get the next inequality

$$\frac{d}{dt}(AR_l(\cdot,t),R_l(\cdot,t))_{s,n} + 2q_0(R_{l2}(\cdot,t),R_{l2}(\cdot,t))_{s,n-m} \leqslant \\ \leqslant 2|(\partial_t^l F(\cdot,t),R_l(\cdot,t))_{s,n}|. \quad (40)$$

The estimations (33) and (34) yield the next estimation

$$|(\partial_t^l F(\cdot,t),R_l(\cdot,t))_{s,n}| \leqslant \varepsilon^{N+1}|(P_1(\partial_t^l V_N(\cdot,t)) + \varepsilon^{-l}L_1(\partial_\tau^l Z_N(\cdot,\tau)), \quad (41)$$

$$R_l(\cdot,t))_{s,n}| + \varepsilon^{N-l}|(L_0(\partial_\tau^l Z_N(\cdot,\tau)) + L_1(\partial_\tau^l Z_{N-1}(\cdot,\tau)),$$

$$A_0 R_l(\cdot,t))_{s,n}| \leqslant \\ \leqslant C(T)(\varepsilon^{N-l}\kappa(t)\|R_{l1}(\cdot,t)\|_{s,m} + (\varepsilon^{N+1} + \kappa(t)\varepsilon^{N+1-l})\|R_l(\cdot,t))\|_{s,n}),$$

where $0 \leqslant t \leqslant T, \tau = t/\varepsilon$ and $\kappa(t) = e^{-q_0 t/\varepsilon}(1+(t/\varepsilon)^N)$. Integrating (40) by t and using (41), we can get the next inequality

$$\|R_{l1}(\cdot,t))\|_{s,m}^2 + \varepsilon\|R_{l2}(\cdot,t))\|_{s,n-m}^2 + 2q_0\int_0^t \|R_{l2}(\cdot,\theta)\|_{s,n-m}^2\,d\theta \leqslant \\ \leqslant \|R_{l1}(\cdot,0)\|_{s,m}^2 + \varepsilon\|R_{l2}(\cdot,0))\|_{s,n-m}^2 + C(T)(\varepsilon^{N-l}\int_0^t \kappa(\theta)\|R_{l1}(\cdot,\theta)\|_{s,m}\,d\theta + \\ + \int_0^t (\varepsilon^{N+1} + \kappa(\theta)\varepsilon^{N-l+1})\|R_l(\cdot,\theta)\|_{s,n}\,d\theta), \quad 0 \leqslant t \leqslant T, \quad (42)$$

We can note that

$$R_l(\cdot,0) = \sum_{\nu=0}^{l-1}(-A^{-1}(B(\partial_x)+D))^{l-\nu-1}A^{-1}\partial_t^\nu F(\cdot,0), \quad l \geqslant 1,$$

and according to (7), $R_0(\cdot,0)=0$.

Therefore, using the equality $A^{-1}A_0=A_0$ and (34), (35), we can find the next estimation

$$\begin{aligned}&\|A^{-1}\partial_t^\nu F(\cdot,0)\|_{s,n}\leqslant\\&\quad\leqslant\varepsilon^{N+1}\|(A^{-1}P_1\partial_t^\nu V_N)(\cdot,0)\|_{s,n}+\varepsilon^{N+1-\nu}\|(A^{-1}L_1\partial_\tau^\nu Z_N)(\cdot,0)\|_{s,n}+\\&\qquad+\varepsilon^{N-\nu}\|A_0(L_0\partial_\tau^\nu Z_N+L_1\partial_\tau^\nu Z_{N-1})(\cdot,0)\|_{s,n}\leqslant\\&\qquad\qquad\leqslant C(T)(\varepsilon^N+\varepsilon^{N-\nu})\leqslant C(T)\varepsilon^{N-\nu},\end{aligned}$$

where $0<\varepsilon<1$, $0\leqslant\nu\leqslant N$.

Thus, we can obtain the next inequalities

$$\begin{aligned}\|R_l(\cdot,0)\|_{s,n}&\leqslant\sum_{\nu=0}^{l-1}\|A^{-1}(B(\partial_x)+D))^{l-\nu-1}A^{-1}\partial_t^\nu F(\cdot,0)\|_{s,n}\leqslant\\&\leqslant C(T)\sum_{\nu=0}^{l-1}\varepsilon^{-(l-\nu-1)}\cdot\varepsilon^{N-\nu}\leqslant C(T)\varepsilon^{N-l+1}.\end{aligned}\tag{43}$$

If the conditions $l<N+1$, $0\leqslant t\leqslant T$, $\varepsilon\ll 0$ are true, we can obtain the estimations

$$\begin{aligned}\int_0^t\kappa(\theta)\|R_{l1}(\cdot,\theta)\|_{s,m}\,d\theta&\leqslant\int_0^t\kappa(\theta)\,d\theta+\int_0^t\kappa(\theta)\|R_{l1}(\cdot,\theta)\|_{s,m}^2\,d\theta\leqslant\\&\leqslant C(T)\varepsilon+\int_0^t\kappa(\theta)\|R_{l1}(\cdot,\theta)\|_{s,m}^2\,d\theta,\end{aligned}\tag{44}$$

and

$$\begin{aligned}&C(T)\int_0^t(\varepsilon^{N+1}+\kappa(\theta)\varepsilon^{N-l+1})\|R_l(\cdot,\theta)\|_{s,n}\,d\theta\leqslant\\&\qquad\leqslant C(T)\varepsilon^{N-l+1}+q_0\int_0^t\|R_{l2}(\cdot,\theta)\|_{s,n-m}^2\,d\theta+\\&\qquad\quad+C(T)\int_0^t(\varepsilon^{N+1}+\kappa(\theta)\varepsilon^{N-l+1})\|R_{l1}(\cdot,\theta)\|_{s,m}^2\,d\theta.\end{aligned}\tag{45}$$

Using the next inequality

$$\begin{aligned}&\|R_{l1}(\cdot,t))\|_{s,m}^2+\varepsilon\|R_{l2}(\cdot,t))\|_{s,n-m}^2+q_0\int_0^t\|R_{l2}(\cdot,\theta)\|_{s,n-m}^2\,d\theta\leqslant\\&\quad\leqslant C(T)(\varepsilon^{N-l+1}+\int_0^t(\varepsilon^{N+1}+\kappa(\theta)\varepsilon^{N-l})\|R_{l1}(\cdot,\theta)\|_{s,m}^2\,d\theta),\ 0\leqslant t\leqslant T,\end{aligned}$$

and the estimations (43), (44), (45), we can find the inequality (42).

Using Gronwall's lemma and the last inequality, we can get the estimations

$$\|R_{l1}(\cdot,t)\|^2_{s,m} \leqslant C(T)\varepsilon^{N-l+1},\ 0 \leqslant t \leqslant T, \tag{46}$$

and

$$\varepsilon\|R_{l2}(\cdot,t)\|^2_{s,n-m} + q_0 \int_0^t \|R_{l2}(\cdot,\theta)\|^2_{s,n-m}\, d\theta \leqslant C(T)\varepsilon^{N-l+1},\ 0 \leqslant t \leqslant T. \tag{47}$$

Using (43) and (47), we can obtain the estimation

$$\begin{aligned}
&\|R_{l2}(\cdot,t)\|^2_{s,n-m} \leqslant \\
&\quad \leqslant \|R_{l2}(\cdot,0)\|^2_{s,n-m} + 2\int_0^t \|R_{l2}(\cdot,\theta)\|_{s,n-m}\|R_{(l+1)2}(\cdot,\theta)\|_{s,n-m}\, d\theta \leqslant \\
&\qquad \leqslant C(T)\varepsilon^{2(N-l+1)} + 2\left(\int_0^t \|R_{l2}(\cdot,\theta)\|^2_{s,n-m}\, d\theta\right)^{1/2} \times \\
&\quad \times \left(\int_0^t \|R_{(l+1)2}(\cdot,\theta)\|^2_{s,n-m}\, d\theta\right)^{1/2} \leqslant C(T)\varepsilon^{N-l+1/2}, \quad 0 \leqslant t \leqslant T.
\end{aligned} \tag{48}$$

The estimates (46) and (48) imply the estimate (39). Therefore, Theorem 1 is proved. □

Thus, we justify asymptotic expansions of the singularly perturbed Cauchy problem (P_ϵ).

5. Conclusions

In this paper we investigate the Cauchy problem for the singularly perturbed Tikhonov-type symmetric system of Fokker–Planck equations. This system consists of non-homogeneous constant coefficients linear parabolic partial differential equations with a small parameter. For these singularly perturbed Cauchy problems a method for constructing asymptotic solutions is proposed. We use the asymptotic method for this Cauchy problem and construct expansions of solutions in the form of decomposition, which has regular and border-layer parts. The asymptotic solutions in the form of regular and boundary-layer parts are obtained and the question of asymptotic solutions behavior when $\varepsilon \to 0$ is investigated. The main result of our work is a justification of an asymptotic expansion for this Cauchy problem. We prove the justification theorem for the asymptotic solutions. Our method can be applied in a wide variety of cases for singularly perturbed Cauchy problems of Fokker–Planck equations. The Fokker–Planck equation is connected with the Chapman–Kolmogorov equation for the transition probability function of a Markov process.

Our results give the approach to investigate the fast-changing processes in liquids and gases, plasma, solid state theory, magnetic, hydrodynamics, radiophysics, telecommunication technology, chemistry, biology, finance and so on. An extension of Fokker–Planck equations with a small parameter to model non-Markovian processes is also possible.

Acknowledgments

This paper has been supported by the RUDN University Strategic Academic Leadership Program and funded by RFBR according to the research projects No. 18-07-00567.

References

[1] D. Daniel, W. T. Taitano, and L. Chacon, “A fully implicit, scalable, conservative nonlinear relativistic Fokker–Planck 0D-2P solver for runaway electrons,” *Computer Physics Communications*, vol. 254, p. 107 361, 2020. DOI: 10.1016/j.cpc.2020.107361.

[2] Y. Ito, “Self-similar orbit-averaged Fokker-Planck equation for isotropic spherical dense star clusters (i) accurate pre-collapse solution,” *New Astronomy*, vol. 83, p. 101 474, 2021. DOI: 10.1016/j.newast.2020.101474.

[3] P. Jiang, “Global existence and large time behavior of classical solutions to the Euler-Maxwell-Vlasov-Fokker-Planck system,” *Journal of Differential Equations*, vol. 268, pp. 7715–7740, 12 2020. DOI: 10.1016/j.jde.2019.11.085.

[4] H. P. Le, “Quantum Fokker-Planck modeling of degenerate electrons,” *Journal of Computational Physics*, vol. 434, p. 110 230, 2021. DOI: 10.1016/j.jcp.2021.110230.

[5] M. A. Malkov, “Propagating Cosmic Rays with exact Solution of Fokker-Planck Equation,” *Nuclear and Particle Physics Proceedings*, vol. 297–299, pp. 152–157, 2018. DOI: 10.1016/j.nuclphysbps.2018.07.023.

[6] W. T. Taitano, L. Chacon, and A. N. Simakov, “An adaptive, implicit, conservative, 1D-2V multi-species Vlasov–Fokker–Planck multi-scale solver in planar geometry,” *Journal of Computational Physics*, vol. 365, pp. 173–205, 2018. DOI: 10.1016/j.jcp.2018.03.007.

[7] H. Wang, “Global existence and decay of solutions for soft potentials to the Fokker–Planck–Boltzmann equation without cut-off,” *Journal of Mathematical Analysis and Applications*, vol. 486, p. 123 947, 2 2020. DOI: 10.1016/j.jmaa.2020.123947.

[8] M. Zanella, “Structure preserving stochastic Galerkin methods for Fokker–Planck equations with background interactions,” *Mathematics and Computers in Simulation*, vol. 168, pp. 28–47, 2020. DOI: 10.1016/j.matcom.2019.07.012.

[9] H. J. Hwang and J. Kim, “The Vlasov–Poisson–Fokker–Planck equation in an interval with kinetic absorbing boundary conditions,” *Stochastic Processes and their Applications*, vol. 129, pp. 240–282, 1 2019. DOI: 10.1016/j.spa.2018.02.016.

[10] H. J. Hwang, J. W. Jang, H. Jo, and J. Y. Lee, "Trend to equilibrium for the kinetic Fokker-Planck equation via the neural network approach," *Journal of Computational Physics*, vol. 419, p. 109 665, 2020. DOI: 10.1016/j.jcp.2020.109665.

[11] S.-N. Li and B.-Y. Cao, "Anomalous heat diffusion from fractional Fokker–Planck equation," *Journal of Computational Physics*, vol. 99, p. 105 992, 2020. DOI: 10.1016/j.aml.2019.07.023.

[12] H. Patel and B. D. Shizgal, "Pseudospectral solutions of the Fokker-Planck equation for Pearson diffusion that yields a Kappa distribution; the associated SUSY Schrodinger equation," *Computational and Theoretical Chemistry*, vol. 1194, p. 113 059, 2021. DOI: 10.1016/j.comptc.2020.113059.

[13] L. Philipp and B. D. Shizgal, "A Pseudospectral solution of a bistable Fokker–Planck equation that models protein folding," *Physica A: Statistical Mechanics and its Applications*, vol. 522, pp. 158–166, 2019. DOI: 10.1016/j.physa.2019.01.146.

[14] Y. Su and L. Yao, "Hydrodynamic limit for the inhomogeneous incompressible Navier-Stokes/Vlasov-Fokker-Planck equations," *Journal of Differential Equations*, vol. 269, pp. 1079–1116, 2 2020. DOI: 10.1016/j.jde.2019.12.027.

[15] A. N. Tikhonov, "The dependence of the solutions of differential equations on a small parameter [O zavisimosti reshenij differencial'nyh uravnenij ot malogo parametra]," *Sbornik: Mathematics [Matematicheskii Sbornik]*, vol. 22 (64), pp. 193–204, 2 1948, in Russian.

[16] M. I. Vishik and L. A. Lyusternik, "Regular degeneration and boundary layer for linear differential equations with a small parameter multiplying the highest derivatives [Regulyarnoe vyrozhdenie i pogranichnyj sloj dlya linejnyh differencial'nyh uravnenij s malym parametrom]," *Russian Mathematical Surveys [Uspekhi matematicheskih nauk]*, vol. 12, pp. 3–122, 5(77) 1957, in Russian.

[17] A. B. Vasil'eva, "Asymptotic behaviour of solutions of certain problems for ordinary non-linear differential equations with a small parameter multiplying the highest derivatives [Asimptotika reshenij nekotoryh zadach dlya obyknovennyh nelinejnyh differencial'nyh uravnenij s malym parametrom pri starshih proizvodnyh]," *Russian Mathematical Surveys [Uspekhi matematicheskih nauk]*, vol. 18, pp. 15–86, 3(111) 1963, in Russian.

[18] S. A. Lomov, "The construction of asymptotic solutions of certain problems with parameters [Postroenie asimptoticheskih reshenij nekotoryh zadach s parametrami]," *Mathematics of the USSR-Izvestiyas [Izvestiya Akademii nauk SSSR]*, vol. 32, pp. 884–913, 4 1968, in Russian. DOI: 10.1070/IM1968v002n04ABEH000675.

[19] V. A. Trenogin, "The development and applications of the asymptotic method of Lyusternik and Vishik [Razvitie i prilozhenie asimptoticheskogo metoda Lyusternika–Vishika]," *Russian Mathematical Surveys [Uspekhi matematicheskih nauk]*, vol. 25, pp. 123–156, 4(154) 1970, in Russian. DOI: 10.1070/RM1970v025n04ABEH001262.

[20] J. L. Lions, "Singular perturbations in boundary problems and optimal control[Perturbations singulieres dans les problems aux limites et al control optimal]," French, *Lecture Notes in Mathematics*, vol. 323, pp. 1–645, 1973. DOI: 10.1007/BFb0060528.

[21] O. Hawamdeh and A. Perjan, "Asymptotic expansions for linear symmetric hyperbolic systems with small parameter," *Electronic Journal of Differential Equations*, vol. 1999, pp. 1–12, 31 1999.

[22] A. Perjan, "Linear singular perturbations of hyperbolic-parabolic type," *Buletinul Academiei de Ştiinţe a Republicii Moldova, Matematica*, pp. 95–112, 2 2003.

[23] A. Gorban, "Model reduction in chemical dynamics: slow invariant manifolds, singular perturbations, thermodynamic estimates, and analysis of reaction graph," *Current Opinion in Chemical Engineering*, vol. 21, pp. 48–59, 2018. DOI: 10.1016/j.coche.2018.02.009.

[24] C. D. Zan and P. Soravia, "Singular limits of reaction diffusion equations and geometric flows with discontinuous velocity," *Nonlinear Analysis*, vol. 200, p. 111 989, 2020. DOI: 10.1016/j.na.2020.111989.

For citation:

M. A. Bouatta, S. A. Vasilyev, S. I. Vinitsky, The asymptotic solution of a singularly perturbed Cauchy problem for Fokker–Planck equation, Discrete and Continuous Models and Applied Computational Science 29 (2) (2021) 126–145. DOI: 10.22363/2658-4670-2021-29-2-126-145.

Information about the authors:

Bouatta, Mohamed A. — PhD's degree student of Department of Applied Probability and Informatics of Peoples' Friendship University of Russia (RUDN University) (e-mail: adelbouatta.rudn@mail.ru, phone: +7(495)9522823, ORCID: https://orcid.org/0000-0002-5477-8710)

Vasilyev, Sergey A. — Candidate of Physical and Mathematical Sciences, Assistant professor of Department of Applied Probability and Informatics of Peoples' Friendship University of Russia (RUDN University) (e-mail: vasilyev_sa@rudn.ru, phone: +7(495)9522823, ORCID: https://orcid.org/0000-0003-1562-0256, ResearcherID: 5806-2016, Scopus Author ID: 56694334800)

Vinitsky, Sergey I. — Leading researcher of Bogolyubov Laboratory of Theoretical Physics of Joint Institute for Nuclear Research, Professor of Department of Applied Probability and Informatics of Peoples' Friendship University of Russia (RUDN University) (e-mail: vinitsky@theor.jinr.ru, phone: +7(49621)65912, ORCID: https://orcid.org/0000-0003-3078-0047, ResearcherID: B-7719-2016, Scopus Author ID: 7003380373)

УДК 517.928.1:517.958:519.633
PACS 02.30.Jr, 02.30.Mv, 11.10.Jj, 05.20.Dd, 05.40.Jc,
DOI: 10.22363/2658-4670-2021-29-2-126-145

Асимптотическое решение сингулярно возмущённой задачи Коши для уравнения Фоккера–Планка

М. А. Буатта[1], С. А. Васильев[1], С. И. Виницкий[1,2]

[1] *Российский университет дружбы народов*
ул. Миклухо-Маклая, д. 6, Москва, 117198, Россия
[2] *Объединённый институт ядерных исследований*
ул. Жолио-Кюри, д. 6, Дубна, Московская область, 141980, Россия

Асимптотические методы — очень важная область прикладной математики. Существует множество современных направлений исследований, в которых используется малый параметр, например статистическая механика, теория химических реакций и др. Использование уравнения Фоккера–Планка с малым параметром очень востребовано, поскольку это уравнение является параболическим дифференциальным уравнением в частных производных, а решения этого уравнения дают функцию плотности вероятности.

В работе исследуется сингулярно возмущённая задача Коши для симметричной линейной системы параболических дифференциальных уравнений в частных производных с малым параметром. Мы предполагаем, что эта система является неоднородной системой тихоновского типа с постоянными коэффициентами. Цель исследования — рассмотреть эту задачу Коши, применить асимптотический метод и построить асимптотические разложения решений в виде двухкомпонентного ряда. Таким образом, это разложение имеет регулярную и погранслойную части. Основным результатом данной работы является обоснование асимптотического разложения для решений этой задачи Коши. Наш метод может быть применён для широкого круга сингулярно возмущённых задач Коши для уравнений Фоккера–Планка.

Ключевые слова: асимптотический анализ, сингулярно возмущённое дифференциальное уравнение, задача Коши, уравнение Фоккера–Планка

Research article

UDC 519.872:519.217
PACS 07.05.Tp, 02.60.Pn, 02.70.Bf
DOI: 10.22363/2658-4670-2021-29-2-146-157

Calculation of special functions arising in the problem of diffraction by a dielectric ball

Ksaverii Yu. Malyshev

Skobeltsyn Institute of Nuclear Physics
Lomonosov Moscow State University
GSP-1, Leninskie Gory, Moscow, 119991, Russian Federation

(received: April 29, 2021; accepted: May 25, 2021)

To apply the incomplete Galerkin method to the problem of the scattering of electromagnetic waves by lenses, it is necessary to study the differential equations for the field amplitudes. These equations belong to the class of linear ordinary differential equations with Fuchsian singularities and, in the case of the Lüneburg lens, are integrated in special functions of mathematical physics, namely, the Whittaker and Heun functions.

The Maple computer algebra system has tools for working with Whittaker and Heun functions, but in some cases this system gives very large values for these functions, and their plots contain various kinds of artifacts. Therefore, the results of calculations in the Maple'11 and Maple'2019 systems of special functions related to the problem of scattering by a Lüneburg lens need additional verification. For this purpose, an algorithm for finding solutions to linear ordinary differential equations with Fuchsian singular points by the method of Frobenius series was implemented, designed as a software package Fucsh for Sage. The problem of scattering by a Lüneburg lens is used as a test case. The calculation results are compared with similar results obtained in different versions of CAS Maple.

Fuchs for Sage allows computing solutions to other linear differential equations that cannot be expressed in terms of known special functions.

Key words and phrases: linear differential equations, Whittaker functions, Heun functions

1. Introduction

The problem of diffraction of a plane electromagnetic wave by a ball with an arbitrary radially symmetric filling allows the construction of an analytical solution by the incomplete Galerkin method [1]. Let us make use of a spherical coordinate system and assume that the dielectric constant of the ball ϵ depends only on r, and the permeability μ is constant. Let us expand the Borgnis potentials u, v for electric- and magnetic-type fields in terms of the system of spherical functions:

$$u = \sum_{n=1}^{\infty} u_n(r) P_n^{(1)}(\theta) \sin\phi, \quad v = \sum_{n=1}^{\infty} v_n(r) P_n^{(1)}(\theta) \sin\phi.$$

Functions $u_n(r)$, $v_n(r)$ satisfy linear differential equations of the second order: for TE-polarized wave

$$\frac{d}{dr}\frac{1}{\mu}\frac{du_n}{dr} + \left[k^2\epsilon - \frac{n(n+1)}{\mu r^2}\right] u_n = 0, \tag{1}$$

and for TM-polarized wave

$$\frac{d}{dr}\frac{1}{\epsilon}\frac{dv_n}{dr} + \left[k^2\mu - \frac{n(n+1)}{\epsilon r^2}\right] v_n = 0. \tag{2}$$

Not only in the classical case of a ball with constant filling, but also in the case of a Lüneburg lens, when

$$\epsilon = \begin{cases} 2 - r^2, & r < 1, \\ 1, & r > 1, \end{cases}$$

these equations are integrated in special functions of mathematical physics. In the classical case, the cylindrical functions are obtained [2]–[4]. For a Lüneburg lens, (1) was integrated in the paper by Lock [5] in terms of Whittaker functions. In the Maple system [6] both equations (1) and (2) for a Lüneburg lens are integrable: the solution to Eq. (1) is expressed in terms of Whittaker functions and the solution to Eq. (2) in terms of Heun functions.

When working with these functions in the Maple system, we faced the fact that they take on huge values that grow indefinitely with an increase in n, and all sorts of artifacts (gaps and ripples) appear in the plots. This observation raised doubts about the adequacy of the algorithms used in Maple.

However, it is easy to see that both equations (1) and (2) are linear differential equations of the 2nd order that have a Fuchsian singular point [7] at $r = 0$. Therefore, their solutions upon the analytic dependence of ϵ on r can be expanded in the Frobenius series [7]. The coefficients of the equations (1) and (2) have finite nonzero singular points only where the functions ϵ and $1/\epsilon$ have them, respectively. In particular, if ϵ is a polynomial, then the Frobenius series for the solution to Eq. (1) converges for all r, and the Frobenius series for the solution of Eq. (2) converges in a circle, on the boundary of which the complex zero with the least modulus lies [7]. For example, in the case of the Lüneburg lens, the Frobenius series for the solution to Eq. (1) converges for all r, and for the solution of Eq. (2), the radius of convergence is $\sqrt{2}$. Therefore, to find the field in the lens, it is quite sufficient to calculate the coefficients of the Frobenius series for the solutions of Eqs. (1) and (2).

2. Fuchs for Sage package

In general, the problem of finding Frobenius series can be formulated as follows: for a linear differential equation

$$x^2y'' + xpy' + qy = 0, \tag{3}$$

with meromorphic functions p, q, construct a solution in the form of a series

$$y = x^r(1 + u_1x + u_2x^2 + \dots),$$

where r is a root of characteristic equation

$$r(r-1) + p(0)r + q(0) = 0. \tag{4}$$

Usually, both roots of this equation correspond to solutions, but in some cases, when choosing a root with a smaller real part, a solution in the form of a series does not exist. In this case, there is one solution in the form of a Frobenius series, and the second solution is obtained from the Liouville formulas connecting two solutions of a second-order linear differential equation [7]. The solution to this problem was implemented in CAS Sage [8], as the Fuchs for Sage software package.

Given symbolic expressions p and q, the function `fuchs_order(p,q)` returns the roots of Eq. (4) as elements of the algebraic number field.

```
sage: load('fuchs.sage')
None
sage: fuchs_order(1,x^2-3^2)
[-3, 3]
sage: fuchs_order(1,x^2-8)
[-2.828427124746190?, 2.828427124746190?]
```

Function `fuchs_order(p,q,r,N)` returns symbolic expression

$$y = x^r(1 + u_1x + u_2x^2 + \dots + u_Nx^N),$$

given symbolic expressions p and q, order r, and number N of the sought series terms.

This function supports operation with non-rational roots:

```
sage: R=fuchs_order(1,x^2-8)
sage: fuchs_series(1,x^2-8,R[1],10)
(-(1.41301303805500?e-9)*x^10 + (2.212333918945947?e-7)*x^8
- 0.00002417081750580247?*x^6 + 0.001690534180537310?*x^4
- 0.06530096874093536?*x^2 + 1)*x^2.828427124746190?
```

Let us give an example of calculating the solution of Eq. (1) for the case of a Lüneburg lens with numerical values of the parameters k, n:

```
sage: k=4
sage: n=3
sage: p=0
sage: q=k^2*x^2*(2-x^2) -n*(n+1)
sage: fuchs_order(p,q)
[-3, 4]
sage: expand(fuchs_series(p,q,4,10))
```

```
-3712/19305*x^14 + 1928/3861*x^12 - 448/429*x^10
+ 164/99*x^8 - 16/9*x^6 + x^4
```

The terms of this series do not form a monotonic sequence (see figure 1), therefore, when summing the series, it is important to take a sufficient number of terms.

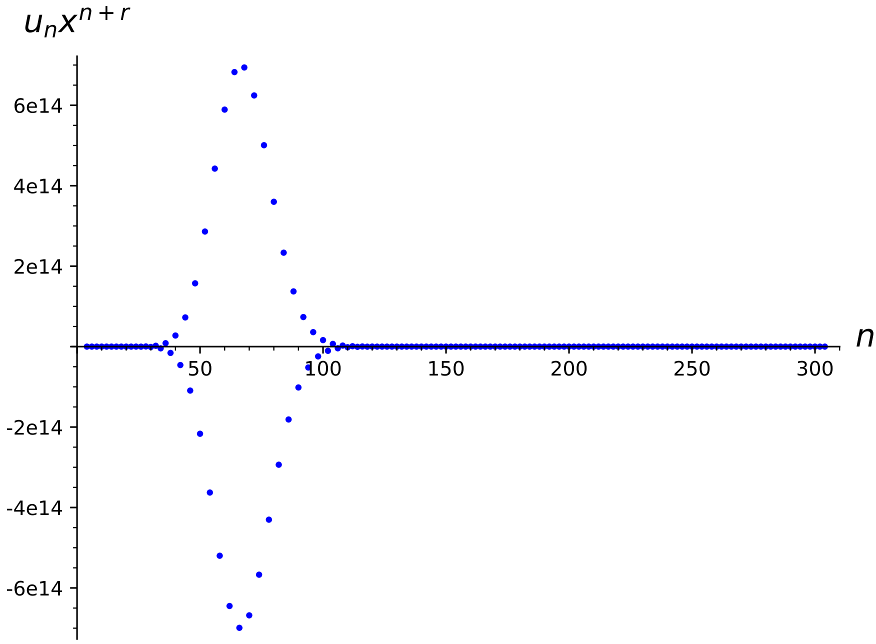

Figure 1. Solution for the Lüneburg lens: distribution of the values of the terms of the series over n — the summand number of the Frobenius series. Calculations are performed for the point $x = 4$

3. Calculation of special functions in the Lüneburg case

Fuchs for Sage allows describing the partial solutions of Eqs. (1) and (2), bounded at zero, in the form of the first N terms of the Frobenius series. In our experiments, a moment was revealed after which a further increase in the number of terms did not lead to a noticeable change in the sum at the reference points. Of course, it would be very convenient to get not greatly overstated theoretical estimates for the number of terms that must be kept in the series in order to preserve the chosen accuracy.

In order to exclude the influence of round-off errors, calculations are carried out in the field of rational numbers, the summation of the series was carried out at rational points of the real axis. For visibility, the rational values obtained without round-off errors are presented in the plots below in logarithmic scale.

Let us compare the results of computer experiments in Sage and Maple for the case of a Lüneburg lens. As noted above, in this case, solutions in the form of a series can be compared with solutions in special functions of mathematical physics that are used in the Maple system.

3.1. TE field

In the case of the Lüneburg lens, the coefficients of Eq. (1) have only two singular points ($r = 0$ and $r = \infty$) and therefore this series can be expressed in terms of the degenerate hypergeometric function or the Whittaker function [9, §13.14] [10]. The Maple system uses the expression

$$u_n = \frac{1}{\sqrt{r}}\mathrm{WhittakerM}\left(\frac{k}{2}, \frac{2n+1}{4}, kr^2\right).$$

This solution to Eq. (1) differs from those obtained using the Frobenius method by the multiplicative constant, which can be found in symbolic form using the Taylor series expansion.

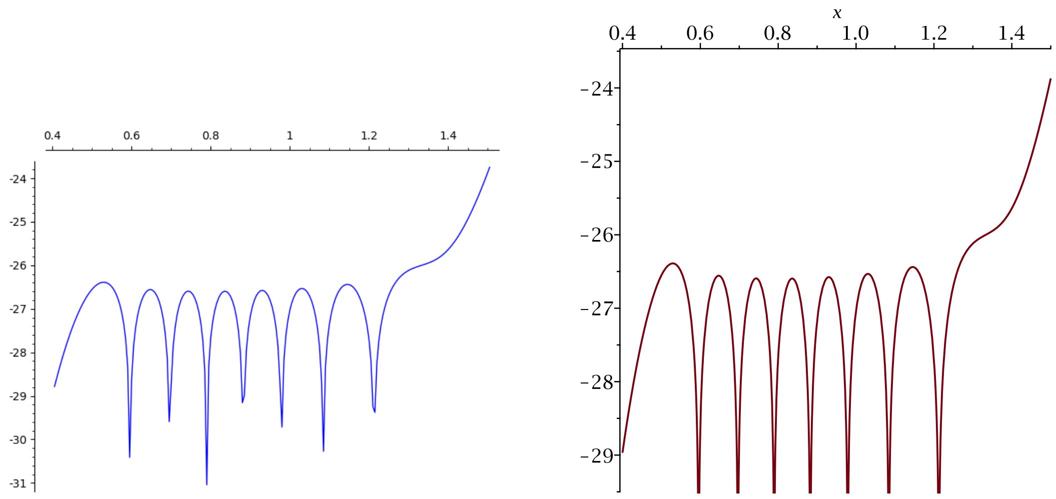

Figure 2. Function $\ln|u_n(x)|$ in case 3, $k = 40$, $n = 25$, plotted in Sage (left) and Maple'2019 (right). In Fuchs for Sage we took 400 terms and the calculations were performed at 221 points

We compared the results of calculating the solution by the Frobenius method and by means of Maple'2019 for 3 representative cases: 1) $k = 4$, $n = 3$, 2) $k = 10$, $n = 3$, 3) $k = 40$, $n = 25$. Despite some difficulties associated with the difference in the automatic selection of proportions of the plots, in all cases the calculation using our package leads to the same results as using Maple, at least with graphic accuracy, see, e.g., figure 2. For a more accurate analysis, we calculated the values at the reference points, see Table 1. It is clearly seen that the values found in Sage and Maple match up to a round-off error. Thus, the numbers to which the Frobenius series converge coincide with the results of the built-in Maple algorithms with high accuracy. Thus, both the algorithm for calculating the Frobenius series and the high orders of magnitude of the sought functions observed in numerical experiments are verified.

Table 1

Values of function $\ln|u_n(x)|$

Case 1: $k = 4$, $n = 3$.

x	$1/2$	1	$3/2$	3
N	50	100	100	200
Sage	-3.21179025713161	-1.66169222058965	-1.32135176796381	8.42740419841879
Maple	-3.211790257	-1.661692220	-1.321351768	8.427404199

Case 2: $k = 10$, $n = 3$.

x	$1/2$	1	$3/2$	3
N	50	100	100	500
Sage	-7.92874739435119	-5.90970510172370	-5.14868973498956	51.3761521918252
Maple	-7.928747395	-5.909705102	-5.148689031	51.37615219

Case 3: $k = 40$, $n = 25$.

x	$1/2$	1	$3/2$	3
N	100	300	400	1000
Sage	-26.5511644045404	-27.0297223651032	-23.8706312720468	79.7748111646792
Maple	-26.55116440	-27.02972236	-23.87063127	79.77481117

Table 2

Values of function $v_n(x)$. Case 1: $k = 10$, $n = 3$

x	1/2	3/4	1	7/5
N	100	100	300	700
Sage	0.000368374895008100	-0.00110378333099445	0.00201228022550062	-0.00181338274195031
Maple	0.0003683748946	-0.001103783338	0.002012279981	-0.001813534799

Table 3

Partial sums of Frobenius series for $v_n(x)$ at the singular point $x = \sqrt{2}$. Case 1: $k = 10$, $n = 3$

N	100	300	700	1000
Sage	-0.00181372503052628	-0.00181282882557290	-0.00181273282789891	-0.00181272165872556

3.2. TM field

Equation (2) has 4 singular points in the complex plane: $r = 0$, $r = \pm\sqrt{2}$, and $r = \infty$. Therefore, its solutions are expressed in terms of the Heun confluent function [9, §31.12] [11]. In Maple the expression

$$v_n = e^{kr^2/2}\mathrm{HeunC}(2k, n + 1/2, -2, k^2, -k^2 + 3/4, r^2/2)r^{n+1} \tag{5}$$

is used. To find the multiplicative constant, by analogy with above, we tried to find the first non-vanishing term of the Taylor series of this function in the vicinity of the point $r = 0$. Unfortunately, the standard function `taylor` cannot be applied to the v_n function for expansion in Taylor series.

Remark. An attempt of using `taylor` to find the first three partial sums of the Taylor series at the point $r = 0$ leads to the result $O(r^4)$. An attempt to find the fourth partial sum at the point $r = 0$ leads to an error `Error, (in series/function) unable to compute series.` We observed this kind of failure in all test examples without exception. When choosing a point other than zero as the center of the expansion, the function `taylor` works without errors.

Nevertheless, computer experiments show that the function (5), calculated in Maple, coincides with a high accuracy with the sum of the Frobenius series, see Table 2. This makes us to assume that the desired constant is 1.

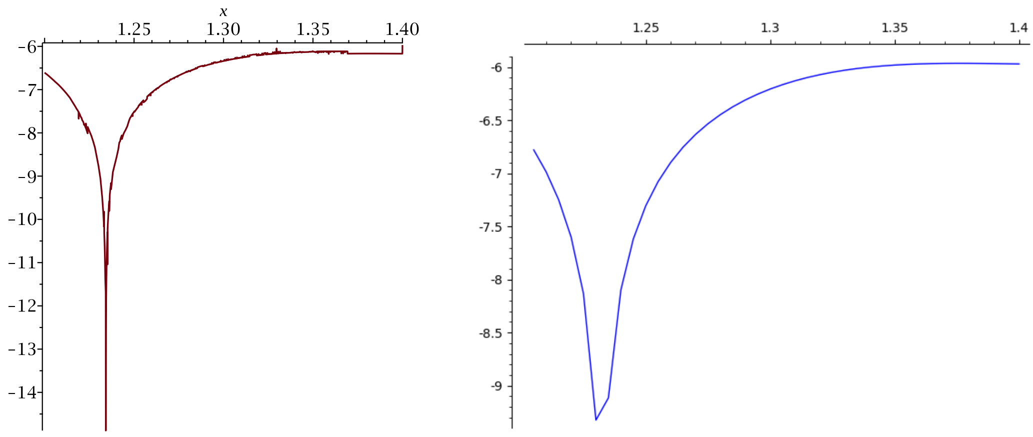

Figure 3. Plot of function $\ln|v_n(x)|$ at $k = 18$, $n = 1$; on the right – Frobenius series with $N = 200$ terms, calculated at 41 points, on the left – plot from Maple'2019

Unlike Eq. (1), Eq. (2) has a finite singular point, namely $x = \sqrt{2}$. We will now show that for $x \geqslant \sqrt{2}$ the Maple system produces incorrect results for representing the function $v_n(x)$.

The Frobenius exponents in the vicinity of the Fuchsian singular point $x = \sqrt{2}$ of Eq. (2) are equal to 0 and 2, and do not depend on the parameters n and k. In the first case, the application of our function leads to division by zero, which indicates the presence of a logarithmic singularity in the expression of the desired function [7], [11]. In this case, the solution corresponding to the Frobenius exponent equal to 0 is bounded at the singular point $x = \sqrt{2}$. In the second case, according to Fuchs theorem [7] we obtain a Frobenius series with a nonzero radius of convergence. Therefore, the function $v_n(x)$ continues analytically beyond the point $x = \sqrt{2}$, having a removable singularity at this point for real values of x. The plot of the Frobenius series sum (figure 3) fully confirms that v_n has a finite limit at the point $x = \sqrt{2}$; it cannot give more, since it diverges at $x > \sqrt{2}$.

A numerical experiment in Fuchs for Sage indicates the convergence of the Frobenius series for the function $v_n(x)$ at the point $x = \sqrt{2}$ in the field of real numbers, see Table 3. However, this convergence is noticeably slower than at rational points $x < \sqrt{2}$.

The situation in Maple looks much less clear. Substitution of the value $x = \sqrt{2}$ in the Maple system yields the result `Float(infinity)+Float(infinity)*I` for all the values of k, n we checked. In this case, the plot of $v_n(x)$, obtained by means of Maple'2019, is cut off at this point. Substitution of values $x > \sqrt{2}$ results in complex numbers of astronomical orders of magnitude, for example `evalf(eval(V, r = 3/2))` yields `-5.630587096*10^12 + (1.389900117*10^15)*I`, for the parameter values $k = 10, n = 3$.

Moreover, when calculating the Heun function in Maple, problems appear that are characteristic of the accumulation of round-off errors when summing a power series. In older versions of Maple, these problems were encountered for all considered parameters, and their first appearance took place already at $k = 10$, see figure 4. In new versions, the same shortcomings in the display of plots appear in a different range of parameters: the highest harmonic $n = 1$ is displayed incorrectly at $k \geqslant 18$ (see figure 3, left, and 5). At the same time, even a relatively small number of terms of the Frobenius series makes it possible to obtain a smooth curve without artifacts, see figure 3, right.

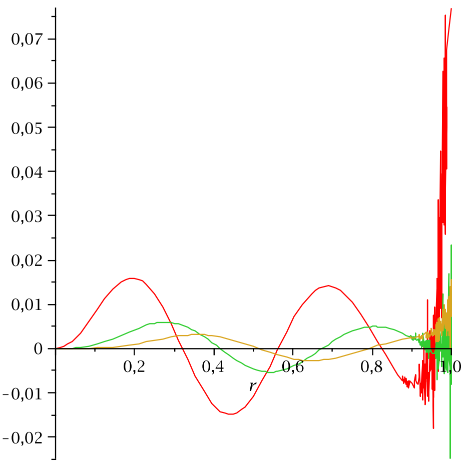

Figure 4. Heun functions v_n for values $k = 10$, $n = 1, 2, 3$ in Maple'11

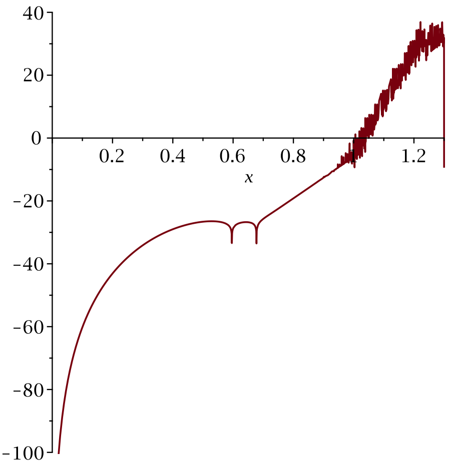

Figure 5. Calculation of functions $\ln |v_n(x)|$. Case 3, $k = 40$, $n = 25$

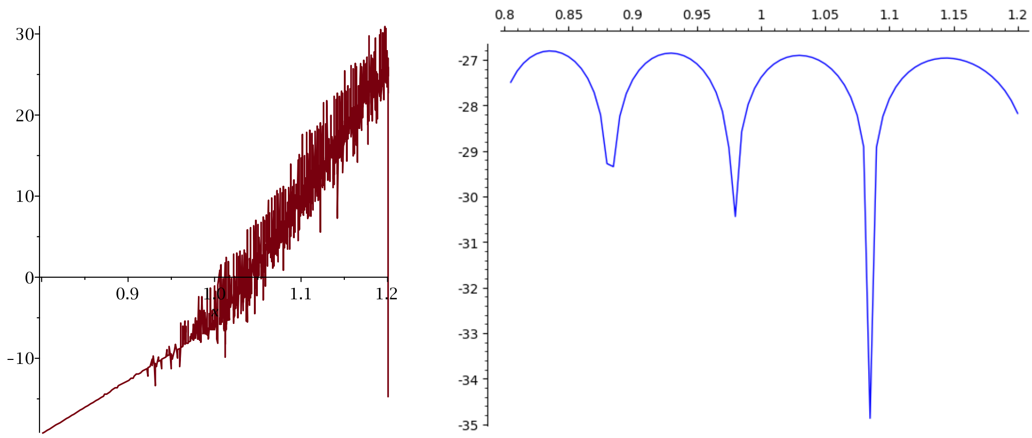

Figure 6. Plot of function $\ln|v_n(x)|$ at $k = 40$, $n = 25$, left — plot from Maple'2019, right — Frobenius series with 250 terms and 82 values of x used

4. Conclusion

In this paper, we present the Fuchs for Sage package , which allows calculating the solutions of second-order equations having the Fuchsian singularity with high accuracy and, in particular, looking for the potentials of the fields scattered by a ball with a wide class of dielectric constant radial dependences. This is confirmed by a comparison with the case of a Lüneburg lens, when the solution is expressed in terms of the known functions of mathematical physics.

At the same time, we made sure in an independent way that the solutions of the equations (1) and (2) in the case of a Lüneburg lens can change by many orders, as it happened in Maple.

The results of our research can be useful for analyzing the electromagnetic field in the vicinity of the focus of the Lüneburg lens [5].

It should be especially noted that the symbolic expression for TM fields in terms of Heun confluent functions found in Maple is dangerous for use, since it gives results that are not completely correct from a theoretical point of view. At the same time, even a small number of terms of the Frobenius series allows good approximations to the values of the sought functions, see figure 6.

Acknowledgments

The author thanks M. D. Malykh (RUDN University) for setting an interesting problem and constant attention to this work. The calculations presented in the article were performed in systems Maple [6] and Sage [8].

References

[1] A. G. Sveshnikov and I. E. Mogilevsky, *Matematicheskiye zadachi teorii difraktsii [Mathematical problems of the theory of diffraction]*. Moscow: MSU, 2010, In Russian.

[2] G. Mie, "Beiträge zur Optik trüber Medien, speziell kolloidaler Metallösungen," *Annalen der Physik*, vol. 25, no. 3, pp. 377–445, 1908. DOI: 10.1002/andp.19083300302.

[3] C. F. Bohren and D. R. Huffman, *Absorption and scattering of light by small particles*. New York: John Wiley & Sons, 1983.

[4] C. Mätzler, *MATLAB Functions for Mie Scattering and Absorption*, Institute of Applied Physics, University of Bern, June 2002. Research Report No. 2002-08 http://arrc.ou.edu/~rockee/NRA_2007_website/Mie-scattering-Matlab.pdf, 2002.

[5] J. Lock, "Scattering of an electromagnetic plane wave by a Luneburg lens. II. Wave theory," *Journal of the Optical Society of America A: Optics Image Science and Vision*, vol. 25, pp. 2980–2990, 2008. DOI: 10.1364/JOSAA.25.002980.

[6] *Waterloo Maple (Maplesoft), Symbolic and numeric computing environment Maple*, https://www.maplesoft.com/, 2019.

[7] F. G. Tricomi, *Differential equations*. London: Blackie & Sons ltd., 1961.

[8] *The Sage Developers, SageMath, the Sage Mathematics Software System (Version 7.4)*, https://www.sagemath.org, 2016.

[9] *National Institute of Standards and Technology (NIST), United States, Digital Library of Mathematical Functions. Version 1.1.1*, https://dlmf.nist.gov, 2021.

[10] A. F. Nikiforov and V. B. Uvarov, *Special Functions of Mathematical Physics. A Unified Introduction with Applications*. Springer Basel AG, 1988.

[11] S. Y. Slavyanov and W. Lay, *Special functions: unified theory based on singularities*. Oxford: OUP, 2000.

For citation:

K. Yu. Malyshev, Calculation of special functions arising in the problem of diffraction by a dielectric ball, Discrete and Continuous Models and Applied Computational Science 29 (2) (2021) 146–157. DOI: 10.22363/2658-4670-2021-29-2-146-157.

Information about the authors:

Malyshev, Ksaverii — engineer, Skobeltsyn Institute of Nuclear Physics, Lomonosov Moscow State University (e-mail: kmalyshev08102@mail.ru, ORCID: https://orcid.org/0000-0001-8823-9136)

УДК 519.872:519.217
PACS 07.05.Tp, 02.60.Pn, 02.70.Bf
DOI: 10.22363/2658-4670-2021-29-2-146-157

О вычислении специальных функций, возникающих при исследовании задачи дифракции на диэлектрическом шаре

К. Ю. Малышев

Научно-исследовательский институт ядерной физики имени Д. В. Скобельцына
Московский государственный университет имени М.В. Ломоносова
Ленинские горы, д. 1, стр. 2, Москва, ГСП-1, 119991, Россия

Для применения неполного метода Галёркина к задаче о рассеянии электромагнитных волн на линзах необходимо исследовать дифференциальные уравнения для амплитуд полей. Эти уравнения принадлежат к классу линейных обыкновенных дифференциальных уравнений с фуксовыми особенностями и, в случае линзы Люнеберга, интегрируются в специальных функциях математической физики — функциях Уиттекера и Гойна.

В системе компьютерной алгебры Maple имеются инструменты для работы с функциями Уиттекера и Гойна, однако в ряде случаев эта система выдаёт очень большие значения для этих функций, а их графики содержат разного рода артефакты. Поэтому результаты вычислений в системах Maple'11 и Maple'2019 специальных функций, связанных с задачей рассеяния на линзе Люнеберга, нуждаются в дополнительной проверке. С этой целью был реализован алгоритм нахождения решений линейных обыкновенных дифференциальных уравнений с фуксовыми особыми точками методом рядов Фробениуса, оформленный в виде пакета программ Fuchs for Sage. Задача рассеяния на линзе Люнеберга используется в качестве тестового примера. Результаты расчётов сопоставляются с аналогичными результатами работы в CAS Maple разных версий.

Пакет Fucsh for Sage позволяет вычислять решения и других линейных дифференциальных уравнений, решения которых не выражаются через известные специальные функции.

Ключевые слова: линейные дифференциальные уравнения, функции Уиттекера, функции Гойна

Research article

UDC 519.872:519.217
PACS 07.05.Tp, 02.60.Pn, 02.70.Bf
DOI: 10.22363/2658-4670-2021-29-2-158-172

To analysis of a two-buffer queuing system with cross-type service and additional penalties

Irina A. Kochetkova[1,2], **Anastasia S. Vlaskina**[1], **Dmitriy V. Efrosinin**[1,3], **Abdukodir A. Khakimov**[1], **Sofiya A. Burtseva**[1]

[1] *Department of Applied Probability and Informatics*
Peoples' Friendship University of Russia (RUDN University)
6, Miklukho-Maklaya St., Moscow, 117198, Russian Federation
[2] *Institute of Informatics Problems, FRC CSC RAS*
44-2, Vavilova St., Moscow, 119333, Russian Federation
[3] *Johannes Kepler Universität Linz*
69, Altenberger Straße, Linz, 4040, Austria

(received: May 20, 2021; accepted: May 25, 2021)

The concept of cloud computing was created to better preserve user privacy and data storage security. However, the resources allocated for processing this data must be optimally allocated. The problem of optimal resource management in the loud computing environment is described in many scientific publications. To solve the problems of optimality of the distribution of resources of systems, you can use the construction and analysis of QS. We conduct an analysis of two-buffer queuing system with cross-type service and additional penalties, based on the literature reviewed in the article. This allows us to assess how suitable the model presented in the article is for application to cloud computing. For a given system different options for selecting applications from queues are possible, queue numbers, therefore, the intensities of transitions between the states of the system will change. For this, the system has a choice policy that allows the system to decide how to behave depending on its state. There are four components of such selection management models, which is a stationary policy for selecting a queue number to service a ticket on a vacated virtual machine each time immediately before service ends. A simulation model was built for numerical analysis. The results obtained indicate that requests are practically not delayed in the queue of the presented QS, and therefore the policy for a given model can be considered optimal. Although Poisson flow is the simplest for simulation, it is quite acceptable for performance evaluation. In the future, it is planned to conduct several more experiments for different values of the intensity of requests and various types of incoming flows.

Key words and phrases: queuing system, cloud computing, Poisson flow, parallel queues, optimal policy

1. Introduction

In order to preserve and protect the users confidential data of computing resources, the concept of *Cloud Computing* was developed as a way to provide secure storage and processing of data for companies and individuals. Cloud Computing includes not only programs and applications delivered as services over the Internet, but also the hardware and system software in the data centers that provide those services. This technology has five main characteristics [1]: on-demand self-service, broad network access, resource pooling, rapid elasticity and measured service. In addition, Cloud Computing includes three main types of services: Infrastructure as a Service, Platform as a Services, and Software as a Service [2]. There are four different ways to use this technology: Public Cloud, Private Cloud, Community Cloud, and Hybrid Cloud.

Nowadays the Cloud Computing model has taken on an increasingly prominent role in a variety of IT-environments, where service providers seek to meet the needs of their customers and improve their competitive position. The increase in the number of users and the expansion of the services provided has led to the need for more storage space. As a result, service providers must work to increase the bandwidth of online data centers. Cloud Computing has become an integral part of maintaining high performance to improve competitiveness [3]. It is the fastest growing technology, and therefore, there are some challenges for developers and for those who use them. Let's consider some tasks:

— tasks of distribution and use of resources;
— model of calculations MapReduce (model of parallel computing over very large amounts of data) [4];
— protection of cloud infrastructure [5];
— ensuring the reliability of the work of many servers [6];
— homomorphic codes (a form of encryption);
— identification of spam pages [7];
— organization of information search.

The problem of optimal resource management in the Cloud Computing environment is described in many scientific publications. As known, one of the approaches to solving this problem is the construction of Queuing Systems (QS). To analyze the distribution of resources and develop an optimal method of performance management, in [8] a multiservice QS of a Cloud Computing model with the same type of tasks and identical servers is investigated. The optimization criterion is the minimization of the ratio of the average queue length to the number of lost tasks. It should be noted that the efficient operation of such a network presupposes the ability to flexibly respond to changes in the demand for computing power by turning on/off machines. Therefore, for a heterogeneous environment of Cloud Computing virtual machines the open Jackson queue network model was proposed in [9], which allows solving the problem of scaling the number of virtual machines. To solve this problem the architecture of an elastic system of dynamic resource management with several queues is presented in [10]. The model of an open system with message queues is presented in [11], where reliability is guaranteed due to the mechanism for optimizing the timeout duration, which does not allow the loss of a single message. The cloud architecture on e-health platforms in medical centers was studied in [12], where a model of two sequential $M/M/s$ queues is proposed: the first assumes receiving services for registration, data verification and consultation, and the second is for accessing the cloud database if the serving server is free. Here, it is possible for tasks to go into orbit, i.e. repeated calls if the service server is busy, and to leave the system due to impatience. The proposed model reduces the overall waiting time by 25% compared to the existing model, and also increases resource efficiency.

We will analyze a two-buffer queuing system with cross-type service and additional penalties. System model describing the trajectory of movement of customers is described in Section 2. Part 3 presents a multidimensional Markov chain. Experimental evaluation of the model is presented in Section 4.

2. System model

2.1. Overview

Let us consider the case presented in Figure 1.

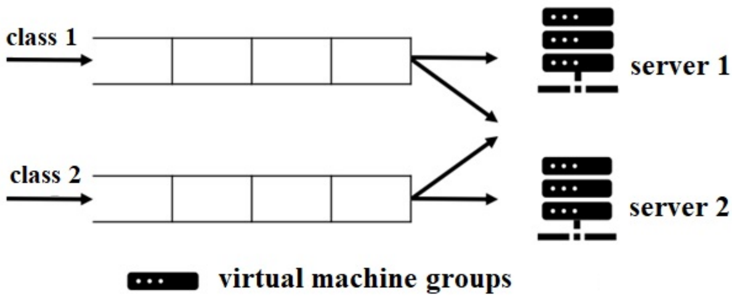

Figure 1. The architecture of two-class multi-server queuing system with a controllable cross-connectivity

In this scenario, two web applications (web apps), classes 1 and 2 in figure, are deployed over the cloud and parallelized on two different services. Each server hosts groups of virtual machines (VM) and each group is assigned to its own class. If the server is not able to provide access to the web apps, the cloud can adapt to network load conditions and another server will provide the necessary resources on demand. In other words, in the system of applied cross-type service, when customers can connect both to the virtual machines of selected server type and to an alternative if there are free virtual machines. If the cloud is not able to provide services, i.e. all virtual machines are busy, the customer will wait for answer. Note that the duration of a service is not related to the type of web apps (class), but is related to a number of server. This scenario of service imposes additional penalties, when customer service on the server assigned to this class of application is cheaper than providing additional resources on an alternative server. It would be logical to assume that it would be more profitable for the cloud provider to leave the customer to wait for the release of resources on his group of virtual machines. But customer waiting also imposes cost losses, downtime of resources, as well as long processing of a request on a low-performance server will be unprofitable factors. As a result, the main idea is to optimally distribute customers between the two servers by calculating the optimal scheme for queue selecting.

2.2. Admission control

In this and the next section consider in more detail how access to virtual machines is performed. With this configuration (as mentioned earlier), the following processes are possible in the operation of the system: receipt of a request from a customer to connect to the cloud, providing access to the first server and providing access to the second server. For the case of receipt of the request:

1. If there are no waiting customers and virtual machines corresponding to this type of request are free, then access to the service can be initiated.
2. If there are no waiting customers, virtual machines corresponding to this type of request are busy, but the alternatives are free, then access to the service can be initiated on alternative server.
3. If all servers are busy, the customer will wait for cloud access in its queue.

2.3. Selection control

The considered system takes into account the cost of providing access to a particular server, therefore it is important to describe the processes that occur when providing a web app on both servers. For the case of providing access to the first server:

1. If there are no waiting customers, then the virtual machines of first server will be idle.
2. If there are first-class waiting customers and there are no second-class waiting customers, then first-class waiting customer will be given access to the first server.
3. If there are no first-class waiting customers and there are second-class waiting customers, then second-class waiting customer will be given access to the first server.
4. If there are all-classes waiting customers, it is necessary to select who will be given access to the first server.

And for the case of providing access to the second server:

1. If there are no waiting customers, then the virtual machines of second server will be idle.
2. If there are second-class waiting customers and there are no first-class waiting customers, then second-class waiting customer will be given access to the second server.
3. If there are no second-class waiting customers and there are first-class waiting customers, then first-class waiting customer will be given access to the second server.
4. If there are all-classes waiting customers, it is necessary to select who will be given access to the first server.

Item 3 reflects the condition of queuing only when all virtual machines are busy. To make the functioning of the system clearer, let's limit the number of virtual machines on each server to one. An example of such system is shown in the Figure 5. In the figure groups of virtual machines (in our case, one

VM on each server) are shown with circles, the different classes are indicated by a filled circle and a shaded circle. A circle within a rectangle represents a waiting customer.

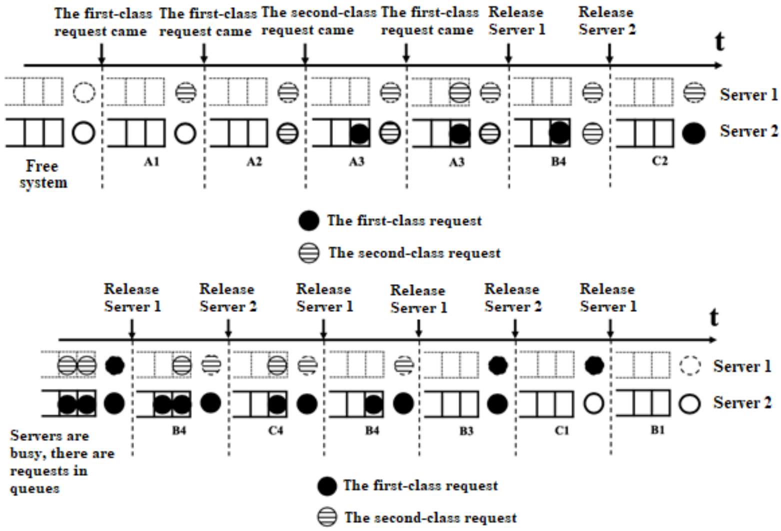

Figure 2. Example of system behavior with one virtual machine on each server

2.4. Problem of finding a routing policy

The step of describing how to access the servers is led to the problem of selection the class of customers when both servers are busy and the system has both types of waiting customers (items 4 in cases of providing access to the servers in previous section are just responsible for this problem). Hence, the question arises - how to define customers who will serviced when the virtual machine is released, i.e. what type of request will be granted access to the cloud. This customer's choice will call *a routing policy*.

There are several methods for organizing and processing queues. We can use the fixed principle or, for example, exhaustive, when we take requests from one queue until it becomes empty then from another until this one becomes empty then we go back to the first, etc. Also we can choose a random principle: from the first, then from the second. Hence, how to choose the routing policy with maximum efficiency?

Therefore, the first thing is to understand the criterion by which to choose the best, i.e. optimal routing policy. The most common problem for models with additional penalties, i.e. which take into account the costs of waiting in queues and servicing on "own" or "alternative" virtual machines, is the problem of minimizing average losses per unit of time. This problem covers special cases of minimizing the average number of requests or the average time in the system. Let's choose the first option as a criterion for routing policy for our study.

And the second thing is how to find this optimal policy: either by brute force, or using a controlled queuing system, the analysis of which allows to find for a given criterion this optimal policy. This algorithm is dynamic and will depend on the state of the system. Those, for each state its own optimal routing policy (some control matrix) can be chosen. This approach allows for a more narrowly configure the system.

3. Queuing model

3.1. Description

The queuing network depicted in Figure 3 models the application of Figure 1.

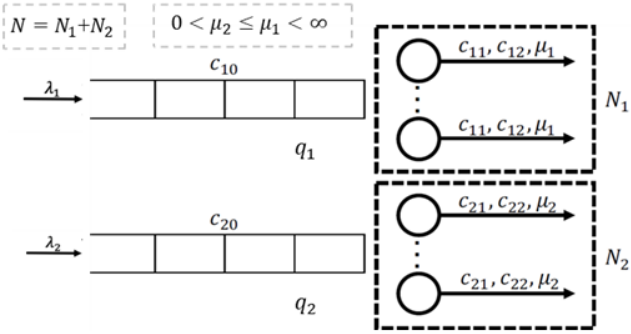

Figure 3. Model in the form of a queuing system

The main parameters of the system are reflected in Table 1. It is composed of two buffers and cross-type service. The system has N_1 and N_2 ($N_1+N_2 = N$, N_k, $k \in \{1, 2\}$) groups of devices, as well as storage units with infinite capacity for the first and second class of customers.Two classes of arrivals are assumed to be generated according a Poisson process with parameters λ_1 and λ_2. The service time is distributed exponentially with intensities μ_1 and μ_2, in such a way that $0 < \mu_2 \leqslant \mu_1 < \infty$. It is also taken into account that one group of devices is more powerful than another. If all groups of devices are busy, the customers arrive in the infinite buffer of its type. The service cost we denote by c_{kj}, where $k \in \{1, 2\}$ is the class of customers and $j \in \{1, 2\}$ is the indicator of our and alternative devices, ($c_{k2} > c_{k1}$): 1 — servicing on our devices, 2 — servicing on an alternative. In other words, c_{11}/c_{21} — cost of servicing on our first/second group devices; c_{12}/c_{22} — cost of servicing on an alternative first/second group devices; c_{k0} ($c_{k0} > 0$) — cost of waiting for service in the k-buffer, $k \in \{1, 2\}$.

3.2. Stochastic process

According the above system description, denote as $Q_k(t)$ — number of customers in the k-buffer at time t and $D_{kj}(t)$ — number of j-customers on k-server at time t. In other words, at some arbitrary time: d_{11} — number of customers of the 1st type on virtual machines of the 1st server, d_{12} — number of customers of the 2nd type on virtual machines of the 1st server, d_{21} — number of customers of the 1st type on virtual machines of the 2nd server, d_{22} — number of customers of the 2nd type on virtual machines of the 2nd server.

So, this system may be modeled by a multidimensional Markov chain with continuous time $\vec{X}(t) = \{Q_1(t), Q_2(t), D_{11}(t), D_{12}(t), D_{21}(t), D_{22}(t)\}$ – the number of customers in the system at t, $t \geqslant 0$ on a state space X:

$$X = \{(\vec{x} = (q_1, q_2, d_{11}, d_{12}, d_{21}, d_{22})) : d_{kj} \geqslant 0, q_k \geqslant 0, k, j = 1, 2; \quad (1)$$
$$(0, 0, d_{11}, d_{12}, d_{21}, d_{22}) : d_{k1} + d_{k2} \leqslant N_k; \quad (2)$$
$$q_1 + q_2 > 0,\ d_{k1} + d_{k2} = N_k, k = 1, 2\}. \quad (3)$$

Table 1

System parameters

Parameters	**Description**
Server	
k	server, $k = \{1; 2\}$
N_k	number of devices (virtual machines) of k-server
μ_k	service intensity of k-server virtual machines (exponential distribution)
Customer and queue	
j	type of arrivals (class of customer), $j = \{1; 2\}$
λ_j	k-th incoming flow rate
Cost	
c_{k0}	cost of waiting in k-customer queue
c_{k1}	cost of k-customer servicing on our devices
c_{k2}	cost of k-customer servicing on alternative devices

3.3. Policy

It is clear that if there are different options for selecting customers from queues then the transition intensity between the states of the system will change. Transition rate matrix can be described in accordance with the rules from in 2.2, 2.3 when $q_1 + q_2 = 0$. And if two queues are occupied, $d_{kj} > 0, q_1 + q_2 \geqslant 1$ (p.4 of 2.3), then in accordance with the queue selection function in a fixed state $\vec{x}$ when servicing j-type customers on k-service:

$$f_{kj}(\vec{x}) \in \{1, 2\}, \quad \vec{x} \in X : q_1 + q_2 > 0. \quad (4)$$

Those the elements are the numbers of the queue from which the customer for the freed device will be taken. Based on the given rules if $q_2 \geqslant 1, q_1 = 0$

then $f_{kj}(\vec{x}) = 2$, if $q_1 \geqslant 1, q_2 = 0$ then $f_{kj}(\vec{x}) = 1$. At $q_1 \geqslant 1, q_2 \geqslant 1$ $f_{kj}(\vec{x})$ is not defined. Besides, this function will depend not only on the current state of the system, but also on the server on which the customer was served. Denote as $\vec{f}(\vec{x}) = (f_{11}(\vec{x}), f_{12}(\vec{x}), f_{21}(\vec{x}), f_{22}(\vec{x}))$ – vector of politics at different values of k, j. We will call the *routing policy* a vector

$$f = \vec{f} = (\vec{f}(\vec{x}), \vec{x} \in X : q_1 + q_2 > 0) \tag{5}$$

of the four components of such selection management models, which is a stationary policy for selecting a queue number to service a customer on a vacated device each time immediately before service ends. It will depend on the server on which the customer was served and what class of customer it is.

Thus, if define a fixed strategy f we can write out the corresponding equilibrium equations system and find the probability distribution. This probability distribution will be denoted as:

$$\pi^f(\vec{x}) = \mathrm{P}[^f(t) = \vec{x}]. \tag{6}$$

3.4. Minimizing cost as optimal policy

Now based on reduction of delays as the selected optimization criterion, it is necessary to compute the service cost for our and alternative devices taking into account waiting in the queue. In some state x it can be represented by:

$$c(\vec{x}) = \sum_{k=1}^{2} (c_{k0}q_k + c_{k1}d_{k1} + c_{k2}d_{k2}). \tag{7}$$

Then the average cost of operating the system for a fixed policy can be described as:

$$g^f = \sum_{\vec{x} \in X} c(\vec{x})\pi^f(\vec{x}). \tag{8}$$

Finally, we will consider the optimal routing policy f^* to be the one that minimizes these values:

$$g^* = \min_f g^f. \tag{9}$$

There is an iterative routing policy algorithm [13] that allows, based on the initial, fixed policy, to construct a sequence of improved policies until the optimal average cost is reached. As a result of performing the described steps, we get matrix of queue selection for each state of the system taking into account the minimization of costs.

4. Simulation model and numerical analysis

4.1. Performance measures

We have studied the properties of a two-buffer queuing system with cross-type service and additional penalties. Performance parameters of this system can be easily found. *The average number of customers of each type in the* *queue*, which is obtained by summing the number of customers in the queue for a fixed routing policy over all system states:

$$\overline{Q}_k = \sum_{\vec{x} \in X} q_k \pi^f(\vec{x}) = \\ = \sum_{q_1=0}^{\infty} \sum_{q_2=0}^{\infty} \sum_{d_{11}+d_{12}=N_1} \sum_{d_{21}+d_{22}=N_2} q_k \pi^f(q_1, q_2, d_{11}, d_{12}, d_{21}, d_{22}). \quad (10)$$

The average number of devices servicing 1 *and* 2 *classes of customers*, which is calculated by summing the number of customers serviced over all system states:

$$\overline{C}_j = \sum_{\vec{x} \in X} (d_{11} + d_{12} + d_{21} + d_{22}) \pi^f(\vec{x}) = \\ = \sum_{q_1+q2=0} \sum_{d_{11}+d_{12}=0}^{N_1} \sum_{d_{21}+d_{22}=0}^{N_2} \sum_{k=0}^{2} (d_{k1} + d_{k2}) \pi^f(q_1, q_2, d_{11}, d_{12}, d_{21}, d_{22}) + \\ + \sum_{q_1+q2>0} \sum_{d_{11}+d_{12}=N_1} \sum_{d_{21}+d_{22}=N_2} (N_1 + N_2) \pi^f(q_1, q_2, d_{11}, d_{12}, d_{21}, d_{22}) . \quad (11)$$

And *the average number of customers in the system*: $\overline{N} = \sum_{j=1}^{2} (\overline{Q}_j + \overline{C}_j)$.

4.2. Simulation model

It has already been shown that the considered routing policy depends on the states of the system. Therefore, it is dynamic, which means that the question arises how this policy (i.e. transition rate matrix) is sensitive to changes in input data. Another issue is the study of the behavior of the model in other distribution laws. If the first question can be solved by a mathematical model, then the second cannot. Therefore, to analyze the studied model we build a simulation model in the *Anylogic* environment.

To simulate the proposed model, we settled on the *AnyLogic* software tool. *AnyLogic* system is based on the use of the object-oriented Java language. This determines the principles for creating, debugging, and deploying simulation models. One of the features of this tool is the ability to flexibly integrate with external programs, in our case, it is msSQL.

Since the selection policy is a fairly large array of data, we load it into an external Database Management System (DBMS) and each time, according to the degree of fullness of the queues, *AnyLogic* sends a request to msSQL. Table 2 lists the elements and their values of the simulator.

Formulated the table of rules is as follows: $(q_1, q_2, d_{11}, d_{12}, d_{21}, d_{22}, f_{11}, f_{12}, f_{21}, f_{22})$ where q_1 and q_2 is current queue status. d_{11} is number of order from their queue d_{12} is number of orders from someone else's queue. d_{21} and d_{22} are similarly. Indicators $(f_{11}, f_{12}, f_{21}, f_{22})$ reflect which queue the request is taken from, where it is denoted by binary values 0 and 1. SQL requests s are written on *selectOutput* elements of the AnyLogic simulator.

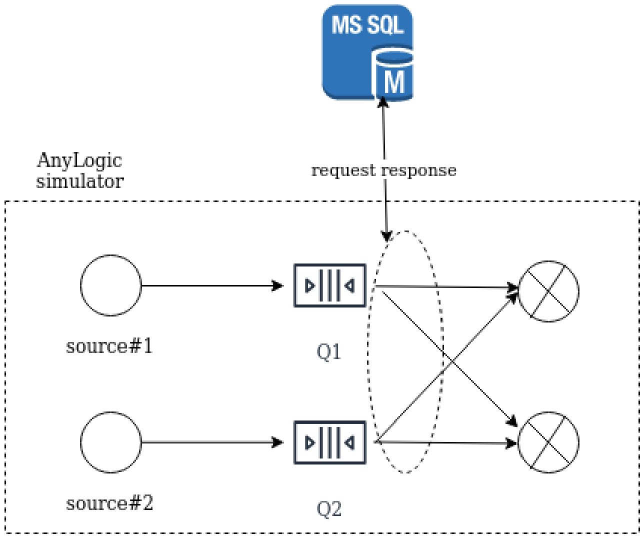

Figure 4. Basic architecture of the simulator

Table 2

Simulation components

Elements	**Value**
source1	input flow
source1	input flow
TS1,TS2,TS,TS3	elements for marking orders with a temporary labels
queue1,queue2	two classes of queues
TE1,TE2	elements for reading labels
selectOutput1,selectOutput2	elements that distribute to instrument groups according to SQL requests
dalay1,delay2	Group of devices
auxiliary variables	
delA	busy state of the first device group
delS	busy state of the second device group
qu1	current state of first queue size
qu2	current state of second queue size

4.3. Numerical example

We start considering requests arriving at rate system with $N_1 = N_2 = 5$ virtual machines on each server. Assume that the incoming flow rates of the 1st and 2nd classes are identical and equal $\lambda_1 = \lambda_2 = 30$. Since the first server is faster then the service intensity in the devices of the first server is $\mu_1 = 20$ and in the second server is $\mu_2 = 5$. The system also has two buffers of infinite capacity. The results of simulation (under exponential assumptions) in the Anylogic environment (Figure 5) are presented in the Table 3. Because the input data for this model is a fixed routing policy then only a fixed case is considered here. Also, the behavior of the system was studied under normal distribution assumptions.

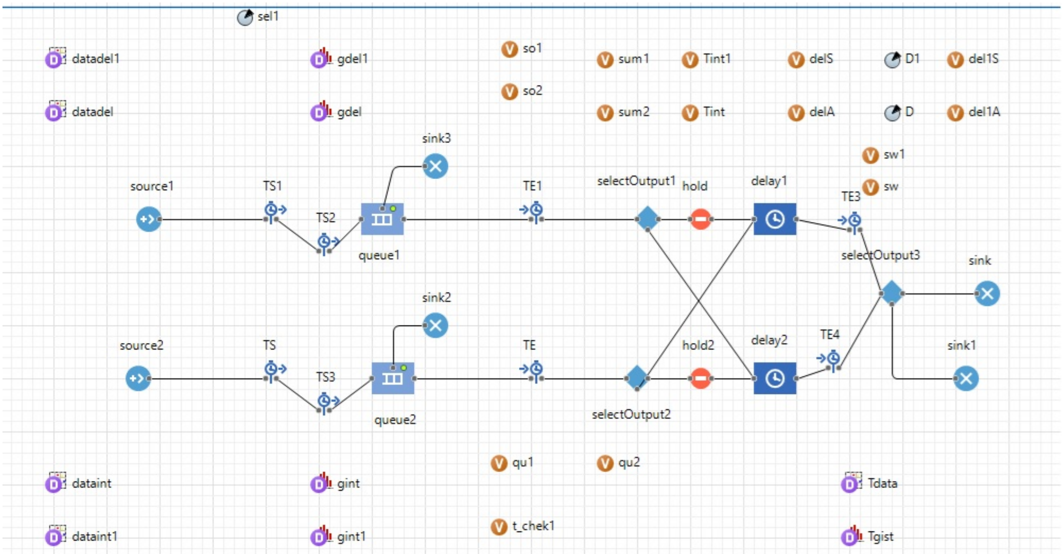

Figure 5. Model schema in Anylogic

The results obtained indicate that requests are practically not delayed in the queue, and therefore the policy for a given model can be considered optimal. Although Poisson flow is the simplest for simulation, it is quite acceptable for performance evaluation.

5. Conclusions

In this paper we analyze the queuing system with two parallel buffers supplied with two groups of servers. A queuing system and a simulation model have been constructed. Initial data were set and the results of the simulation model were obtained. The results obtained indicate that requests are practically not delayed in the queue of the presented QS, and therefore the policy for a given model can be considered optimal. Although Poisson flow is the simplest for simulation, it is quite acceptable for performance evaluation. In the future, it is planned to conduct several more experiments for different values of the intensity of requests and various types of incoming flows.

Table 3

Simulation results

Key Performance Indicators	**Exp (30)**	**Norm (30, 0.001)**	**Norm (30, 0.01)**
Average 1-queue length	0.206	0.289	0.163
Average 2-queue length	0.153	0.168	0.121
Average number of customers serviced on the 1st group of virtual machines	3.85	3.87	3.32
Average number of customers serviced on the 2nd group of virtual machines	3.91	3.94	3.41
Average number of 1-class customers in the system	4.11	4.18	3.68
Average number of 2-class customers in the system	04.08	4.10	3.531
Average time of 1-class of waiting customers	0.007	0.008	0.005
Average time of 2-class of waiting customers	0.005	0.004	0.004
Average time in the system of customers serviced on the 1st group of virtual machines	0.0503	0.0503	0.0402
Average time in the system of customers serviced on the 2nd group of virtual machines	0.199	0.199	0.169
Average time in the system of 1-class customers	0.068	0.070	0.059
Average time in the system of 2-class customers	0.133	0.135	0.124

Acknowledgments

This paper has been supported by the RUDN University Strategic Academic Leadership Program (recipients Irina Kochetkova, Anastasia Vlaskina, simulation model). The reported study was funded by RFBR, project number 20-37-70079 (recipients Irina Kochetkova, Anastasia Vlaskina, Sofia Burtseva, mathematical model).

References

[1] M. Armbrust, A. Fox, R. Griffith, A. D. Joseph, R. Katz, A. Konwinski, and M. Zaharia, "A view of cloud computing," *Communications of the ACM*, vol. 4, no. 53, pp. 50–58, 2010. DOI: 10.1145/1721654.1721672.

[2] N. Taleb and E. A. Mohamed, "Cloud computing trends: a literature review," *Academic Journal of Interdisciplinary Studies*, vol. 1, no. 9, pp. 91–104, 2020. DOI: 10.36941/ajis-2020-0008.

[3] I. Baldini, P. Castro, K. Chang, P. Cheng, S. Fink, V. Ishakian, and P. Suter, "Serverless computing: current trends and open problems," *Research Advances in Cloud Computing*, pp. 1–20, 2017. DOI: 10.1007/978-981-10-5026-8_1.

[4] V. Sontakke and R. B. Dayanand, "Optimization of Hadoop MapReduce Model in cloud Computing Environment," Proceedings of the 2nd International Conference on Smart Systems and Inventive Technology, ICSSIT 8987823, 2019, pp. 510–515. DOI: 10.1109/ICSSIT46314.2019.8987823.

[5] A. Yashwanth Reddy and R. P. Singh, "Design and development of multi tenancy in cloud: security issues," *International Journal of Scientific and Technology Research*, vol. 3, no. 9, pp. 694–697, 2020.

[6] B. Kalyani and K. Rao, "Assessment of physical server reliability in multi cloud computing system," AIP Conference Proceedings 1952,020045, 2018. DOI: 10.1063/1.5032007.

[7] Y. Li, Y. Xu, and J. Chen, "Research on spam pages identification in search service based on cloud computing," *Huazhong Keji Daxue Xuebao (Ziran Kexue Ban)/Journal of Huazhong University of Science and Technology (Natural Science Edition)*, vol. 1, no. 40, pp. 249–253, 2012.

[8] A. Madankan, A. Delavarkhalafi, S. M. Karbassi, and F. Adibnia, "Resource allocation in cloud computing via optimal control to queuing system," *Bulletin of the South Ural State University, Series: Mathematical Modelling, Programming and Computer Software*, vol. 4, no. 12, pp. 67–81, 2019. DOI: 10.14529/mmp190405.

[9] C. N. Khac, K. B. Thanh, H. H. Dac, S. N. Hong, V. P. Tran, and H. T. Cong, "An Open Jackson Network Model for Heterogeneous Infrastructure as a Service on Cloud Computing," *International Journal of Computer Networks and Communications*, vol. 1, no. 11, pp. 63–80, 2019. DOI: 10.5121/ijcnc.2019.11104.

[10] Z. Cheng, H. Li, Q. Huang, Y. Cheng, and G. Chen, "Research on elastic resource management for multi-queue under cloud computing environment," *Journal of Physics: Conference Series*, vol. 9, no. 898, 2017. DOI: 10.1088/1742-6596/898/9/092003.

[11] L. Jing, C. Yidong, and M. Yan, “Modeling Message Queueing Services with Reliability Guarantee in Cloud Computing Environment Using Colored Petri Net,” *Mathematical Problems in Engineering*, 2015. DOI: 10.1155/2015/383846.

[12] S. Kannan and S. Ramakrishnan, “Performance Analysis of Cloud Computing in Healthcare System Using Tandem Queues,” *International Journal of Intelligent Engineering and Systems*, vol. 4, no. 10, pp. 256–264, 2017. DOI: 10.22266/ijies2017.0831.27.

[13] D. Efrosinin, I. Gudkova, and N. Stepanova, “Algorithmic analysis of a two-class multi-server heterogeneous queuing system with a controllable cross-connectivity,” *Lecture Notes in Computer Science*, vol. 12023, 2020. DOI: 10.1007/978-3-030-62885-7_1.

For citation:

I. A. Kochetkova, A. S. Vlaskina, D. V. Efrosinin, A. A. Khakimov, S. A. Burtseva, To analysis of a two-buffer queuing system with cross-type service and additional penalties, Discrete and Continuous Models and Applied Computational Science 29 (2) (2021) 158–172. DOI: 10.22363/2658-4670-2021-29-2-158-172.

Information about the authors:

Kochetkova, Irina A. — Candidate of Physical and Mathematical Sciences, assistant professor of Department of Applied Probability and Informatics of Peoples’ Friendship University of Russia (RUDN University); Senior Researcher of Institute of Informatics Problems of Federal Research Center “Computer Science and Control” Russian Academy of Sciences (e-mail: gudkova-ia@rudn.ru, phone: +7(495)9550927, ORCID: https://orcid.org/0000-0002-1594-427X, ResearcherID: E-3806-2014, Scopus Author ID: 35332169400)

Vlaskina, Anastasia S. — PHD student of Department of Applied Probability and Informatics of Peoples’ Friendship University of Russia (RUDN University) (e-mail: vlaskina.anastasia@yandex.ru, ORCID: https://orcid.org/0000-0001-6453-814X, Scopus Author ID: 57204395118)

Efrosinin, Dmitriy V. — Doctor of Science in physics and mathematics, associate professor of Johannes Kepler Universitaet Linz; associate professor of Peoples’ Friendship University of Russia (RUDN University) (e-mail: dmitry.efrosinin@jku.at, ORCID: https://orcid.org/0000-0002-0902-6640)

Khakimov, Abdukodir A. — Junior researcher of Department of Applied Probability and Informatics of Peoples’ Friendship University of Russia (RUDN University) (e-mail: khakimov-aa@rudn.ru, ORCID: https://orcid.org/0000-0003-2362-3270)

Burtseva, Sofiya A. — Master student of Department of Applied Probability and Informatics of Peoples’ Friendship University of Russia (RUDN University) (e-mail: sofiya_burceva@inbox.ru, ORCID: https://orcid.org/0000-0003-4305-7050)

УДК 519.872:519.217
PACS 07.05.Tp, 02.60.Pn, 02.70.Bf
DOI: 10.22363/2658-4670-2021-29-2-158-172

К анализу двухбуферной системы массового обслуживания с кросс-типом обслуживания и дополнительными штрафами

И. А. Кочеткова[1,2], А. С. Власкина[1], Д. В. Ефросинин[1,3], А. А. Хакимов[1], С. А. Бурцева[1]

[1] *Кафедра прикладной информатики и теории вероятностей*
Российский университет дружбы народов
ул. Миклухо-Маклая, д. 6, Москва, 117198, Россия
[2] *Институт проблем информатики*
Федеральный исследовательский центр «Информатика и управление» РАН
ул. Вавилова, д. 44, корп. 2, Москва, 119333, Россия
[3] *Линцский университет*
Альтенбергерштрассе, д. 69, Линц, Австрия, 4040

Концепция облачных вычислений была создана для улучшения конфиденциальности пользователей и безопасности хранения данных. Однако ресурсы, выделяемые для обработки этих данных, должны быть правильно распределены. Проблема оптимального управления ресурсами в среде облачных вычислений описана во многих научных публикациях. Для решения задач оптимальности распределения ресурсов систем можно использовать построение и анализ характеристик СМО. Авторами проведён анализ системы массового обслуживания с двумя очередями с кросс-типом обслуживания и дополнительными штрафами, который основывается на литературных источниках, рассмотренных в статье. Это позволяет нам оценить, насколько модель, представленная в статье, подходит для применения в облачных вычислениях. Данная система предполагает разные варианты выбора заявок из очередей, номеров очередей, следовательно, интенсивности переходов между состояниями системы будут меняться. Для этого предлагается политика выбора, которая позволяет системе решать, как себя вести в зависимости от своего состояния. Используются четыре компоненты модели управления выбором, которые представляют собой стационарную политику для определения номера очереди, из которой будет взята заявка на обслуживание. Данный выбор происходит каждый раз непосредственно перед окончанием обслуживания. Для численного анализа построена имитационная модель.

Ключевые слова: система массового обслуживания, облачные вычисления, пуассоновский поток, параллельные очереди, оптимальная политика